

Technical Report 95-376

Absorbing Boundary Conditions for the Schrödinger Equation

Thomas Fevens Hong Jiang

February 16, 1995

The research of the first author was supported in part by an Information Technology Research Centre bursary. Research of the second author was supported in part by the Natural Sciences and Engineering Research Council of Canada.

Abstract. A large number of differential equation problems which admit traveling waves have very large (typically infinite) naturally defined domains, with boundary conditions defined at the domain boundary. To be able to numerically solve these problems in smaller subdomains of the original domain, artificial boundary conditions must be defined for these subdomains. One such artificial boundary conditions which can minimize the size of such subdomains are absorbing boundary conditions. A technique used to reduce the necessary spatial domain when numerically solving partial differential equations that admit traveling waves is the imposition of absorbing boundary conditions. Such absorbing boundary conditions have been extensively studied in the context of hyperbolic wave equations. A general absorbing boundary condition will be developed for the Schrödinger equation with one spatial dimension, using group velocity considerations. Previously published absorbing boundary conditions will be shown to reduce to special cases of this absorbing boundary condition. The well-posedness of the Initial Boundary Value Problem of the absorbing boundary condition, coupled to the interior Schrödinger equation, will also be discussed. Extension of the general absorbing boundary condition to higher spatial dimensions is demonstrated. Numerical simulations using initial single Gaussian, double Gaussian and Pseudo-delta function distributions will be given, with comparison to exact solutions, to demonstrate the reflectivity properties of various orders of the absorbing boundary condition.

Key words. Schrödinger Equation, Absorbing Boundary Conditions, Radiation Boundary Conditions, Initial-Boundary Value Problems

AMS subject classifications. 35L35, 65M99, 35A40

1. Introduction . A large variety of numerical calculations involving the solutions to partial differential equations require the imposition of artificial boundary conditions to delimit the computational domain to a manageable size. This often happens when the natural domain for the problem being solved is infinite and thus the natural boundary conditions for the problem are defined at infinity. But if we desire the numerical solution on only a finite section of the domain, the use of artificial boundary conditions is necessitated. It is a requirement of such artificial boundary conditions to not adversely affect the numerical calculation in the interior domain. Specifically, we will consider problems where traveling waves are present.

If standard Dirichlet or Neumann boundary conditions are used for our artificial boundary conditions, then in many cases, a traveling wave evolved via a wave equation will view the boundary condition as an impenetrable barrier and the wave would be completely reflected back into the interior domain. Obviously, this boundary condition would not serve our purposes since the reflected wave would disrupt the interior solution. The only way that such a boundary condition could be used would be to place the boundary condition at a large distance from the relevant interior solution, such that the reflected wave would not effect the interior solution until a large number of time steps (before which the solution would be obtained). This approach would be costly for multi-dimensional problems or problems evolving over many time steps. It would be preferable to use artificial boundary conditions which do not affect the interior solution but which don't have to be removed to a large distance from the relevant interior solution.

Since the boundary condition must be coupled with the interior solution, the boundary condition must be well-posed with respect to the interior solution, and the boundary condition must be stable, such that the numerical solution will remain bounded. Also the artificial boundary condition should annihilate all incident waves such as to produce no reflections which will then propagate into the interior domain. Boundary conditions which satisfy all these conditions are called absorbing (or open, or radiation, or transparent) boundary conditions. The use of absorbing boundary conditions allows for the numerical solution of problems involving traveling waves with a minimal number of spatial points while maintaining the accuracy desired for the solution. This can result in problems being solved more quickly, and allow for the solution of more complex problems, especially in higher dimensions.

In this paper, we will review the previous work that has been done with respect to absorbing boundary conditions for wave equations and similar differential equations. Then we will introduce the Schrödinger equation for which we will develop absorbing boundary conditions. We will discuss previously considered absorbing boundary conditions for the Schrödinger equation and then derive a new absorbing boundary condition. We will show that the previously published absorbing boundary conditions reduce to special cases of the new absorbing boundary condition. We will consider the well-posedness properties of the Initial Boundary Value Problem of the Schrödinger equation coupled to the absorbing boundary condition. Also, we will outline how the general absorbing boundary condition can be extended higher dimensional problems. Finally, we will use a finite difference scheme to solve the Schrödinger equation, and consider the properties of several numerical simulations, using various orders of the absorbing boundary condition.

2. Review of Absorbing Boundary Conditions . In this section, we will consider previous work that has been done to devise absorbing boundary conditions for various wave equations. Absorbing boundary conditions may be divided into

boundary conditions for dispersive or non-dispersive equations. A dispersive equation is one that admits plane wave solutions of the form $e^{-i(\omega t - kx)}$, and the speed of propagation of the wave is partially, or completely, a function of the wave number k . For solutions for a given wave equation, ω is a function of k and is called the *dispersion relation* for the differential equation. The dispersion relation allows us to define the phase speed, $c(k) = \frac{\omega(k)}{k}$, of individual waves, and the group velocity, $C(k) = \frac{d\omega}{dk}(k)$ of wave packets. Energy, for instance, travels with group velocity. Although a differential equation may be non-dispersive (for example, the scalar wave equation) its discretization will nearly always be dispersive [41], so we will consider only dispersive equations. We will review work that has been done to devise absorbing boundary conditions for particular differential equations, exploiting these properties and other properties of dispersive equations.

2.1. Absorbing Boundary Conditions for Wave Equations. A fundamental requirement of an absorbing boundary condition is that the interior solution that is generated is close to the same unique solution as that produced if the boundary conditions were placed at a large distance (say, infinity) from the interior region. For interior schemes involving traveling waves, then the absorbing boundary condition must have the ability to absorb waves incident on it rather than reflecting them back into the interior of the domain.

2.1.1. Damping Regions. The earliest approaches to developing such boundaries used a narrow region extended past the required boundary where dissipation is added to the wave equation [25]. Then the wave impinging on the boundary is damped on the way into the region, reflected by a conventional boundary condition at the end of the appended region, and further damped on the way out. The minimum width of the region must be the width of several of the longest wavelengths to be effective. Therefore, this method can be costly in terms of space and time requirements to implement, especially in higher dimensional problems.

2.1.2. Sommerfeld Radiation Boundary Condition. In 1949, Sommerfeld defined the condition of radiation as “the sources must be sources, not sinks of energy. The energy which is radiated from these sources must scatter to infinity; no energy may be radiated from infinity into ... the field” [40,p.189], thus defining a “radiation boundary condition”. A number of researchers have put Sommerfeld’s absorbing boundary condition in mathematical form for wave equations

$$(1) \quad \frac{\partial u}{\partial t} + c^* \frac{\partial u}{\partial x} = 0,$$

where u is the solution we are seeking in the interior of the computational domain, c^* is some effective phase velocity, and (1) is applied at the $x = L$ right-hand boundary. A number of approaches were considered to determine the optimal value for c^* to minimise reflections. Pearson considered gravity wave propagation in stratified flow where c^* is a function of wavelength [35]. Pearson suggested fixing c^* to the Doppler-shifted phase speed of the dominant vertical mode. Another approach was suggested by Orlanski of calculating c^* from a point just within the boundary at each time step, using a “floating phase velocity” approach [34]. “Floating” implies that the c^* used changes value with respect to the measured phase speed of the incident wave at the boundary. Miller and Thorpe expanded on this “floating phase velocity” approach with higher order approximations to c^* [32] whereas Hedley and Yau used Orlanski’s

original calculation of the floating phase velocity but added constraints on the value of c^* to avoid instabilities [13].

The Sommerfeld radiation boundary condition was expanded to two dimensions by Raymond and Kuo with

$$(2) \quad \frac{\partial u}{\partial t} + c_x^* \frac{\partial u}{\partial x} + c_y^* \frac{\partial u}{\partial y} = 0,$$

where c_x^* and c_y^* are the x and y components of the phase velocity [36]. Also Lick *et al.* generalised the Sommerfeld boundary condition to allow for partial reflection and incoming disturbances (from exterior to the domain) for wave equations in one [28] and two dimensions [29].

Lindman considered a further variation of the Sommerfeld radiation boundary condition of the form

$$\frac{\partial u}{\partial t} + c_x^* \frac{\partial u}{\partial x} = 2 \frac{\partial S}{\partial t} - \frac{c_x^*}{\Delta x} \sum_{n=1}^N h_n,$$

on the $x = 0$ boundary where S is a source function which generates waves into the domain and the h_n 's are correction functions to the absorbing boundary condition which are functions of past data on the boundary, tailored to minimise reflections for incident waves at different angles to the normal of the boundary [30]. This necessitates the updating of up to N functions on the boundary at each time step.

2.1.3. Engquist and Majda Approach. In their paper [5], Engquist and Majda proposed a pseudo-differential operator which acts as a perfectly absorbing boundary condition for the scalar wave equation,

$$(3) \quad \frac{\partial^2 u}{\partial t^2} - \frac{\partial^2 u}{\partial x^2} - \frac{\partial^2 u}{\partial y^2} = 0,$$

with the related dispersion relation

$$(4) \quad \omega^2 = k^2 + l^2.$$

The exact absorbing boundary condition is obtained by inverting this dispersion relation to get an expression for k ,

$$(5) \quad k = \pm \sqrt{\omega^2 - l^2} = \pm \omega \sqrt{1 - l^2/\omega^2}.$$

If the positive branch of this equation is chosen and a mapping is made between the dual of a variable and its related differential operator (via a Fourier transform which involves integrating over all possible values of the duals), the result is a pseudo-differential equation which applied to the $x = L$ boundary which would perfectly absorb all right-traveling waves impinging on the boundary. But since the pseudo-differential form of the absorbing boundary condition is non-local and thus not directly implementable in a finite-difference scheme, Engquist and Majda derive local approximations to Equation (5) by expanding out the square root into terms of the Padé series, to various orders of accuracy. For example, using the approximation $\sqrt{1 - \frac{l^2}{\omega^2}} = 1 + O(\frac{l^2}{\omega^2})$ for the square root in Equation (5), and mapping (via a Fourier transform) the duals to their respective differential forms yields

$$(6) \quad \left(\frac{\partial}{\partial x} - \frac{\partial}{\partial t} \right) u|_{x=0} = 0.$$

as a first approximation to the perfectly absorbing boundary condition whose symbol¹ is given in (5). Note the equivalence of this absorbing boundary condition to those of the Sommerfeld radiation boundary condition (1) with $c^* = -1$. A hierarchy of local absorbing boundary conditions may be derived using higher order approximations. In a second paper, Engquist and Majda introduce a two-dimensional version of their approximations based on an expression in the angle of the wave measured with respect to the normal of the boundary [6].

Durran *et al.* [4] recently compared the floating phase velocity approach of Orlanski [34] and Hedley and Yau [13] with that of Engquist and Majda [5], and found that the latter gave better results for the simulations of a one-dimensional shallow-water flow model and a two-level shallow-water model.

Clayton and Engquist consider absorbing boundary conditions for the acoustic wave equation. They consider an interpolation of the dispersion relation for the acoustic wave equation to develop rational expressions which can be applied at the boundary [3]. The use of a number of different interpolation points in the approximation of the dispersion relation permits the better absorption of more complex impinging waves composed of a number of dominant phase velocities to the boundary as compared with the Padé series using a single interpolation point, which will ideally absorb only one component. Approximating the duals (k_x, k_z, ω) by their corresponding differential operators leads to an explicit differential equation which can be discretized and applied to the boundary, with good results. Although Clayton and Engquist's approach allows for flexible interpolation of the dispersion relation, their solution lacks a general approach of derivation.

Israeli and Orszag consider the idea of mixing damping regions with absorbing boundary conditions [21]. The damping regions act to reduce the amplitude of the outgoing waves as well as any waves that are reflected by the absorbing boundary condition at the end of the damping region. Although this approach combines the general reduction properties of the damping region, with the more specific elimination properties of the absorbing boundary conditions, but there is still a trade-off with respect to the extra grid points which have to be solved at each time step.

2.1.4. Bayliss and Turkel Approach. Bayliss and Turkel consider another approach to develop high order absorbing boundary conditions [1]. Bayliss and Turkel define the following operator

$$(7) \quad B_m = \prod_{l=1}^m \left(L + \frac{2l-1}{r} \right),$$

where

$$(8) \quad L = \frac{\partial}{\partial t} + \frac{\partial}{\partial r}.$$

Then it follows that $B_m p = O(1/r^{2m+1})$, leading them to define the following absorbing boundary condition $B_m p = 0$. Note that this boundary condition becomes asymptotically more accurate as $r \rightarrow \infty$. In two-dimensional Cartesian coordinates, (8) has the form $L = \frac{\partial}{\partial t} + a \frac{\partial}{\partial x} + b \frac{\partial}{\partial y}$, $a^2 + b^2 = 1$, $a > 0$, analogous to the radiation boundary condition of Equation (2).

¹ A symbol is the dual form of a differential equation for the absorbing boundary condition, or equivalently, its dispersion relation.

2.1.5. Canonical Absorbing Boundary Conditions. Higdon showed that the higher order approximations to (5) with their accompanying substitutions of corresponding differential operators ($i\omega \rightarrow \frac{\partial}{\partial t}$, etc.), may be expressed in the following canonical form [14] [16],

$$(9) \quad \left[\prod_{j=1}^p \left(\frac{\partial}{\partial x} - (\cos \alpha_j) \frac{\partial}{\partial t} \right) \right] u|_{x=0} = 0.$$

This canonical form reduces to Engquist and Majda's boundary conditions, based on Padé approximations, when $\alpha_j = 0$. Further, the relationship between Engquist and Majda's higher-order approximations and Bayliss and Turkel's general boundary condition (7) is revealed by the product form of (9). Boundary conditions of this form were also derived independently by Keys [24]. Higdon was able to generalise Engquist and Majda's approximations of the exact absorbing boundary condition (5) in two important ways. First, he showed that Engquist and Majda's approximations could be factorized into first order differential operators, similar to approximation (6). Further, he generalised the factors such that they would annihilate waves incident on the boundary at any angle, rather than optimally at the normal. This more general form greatly simplifies implementation and stability analysis.

Another approach, using group velocity, to derive absorbing boundary conditions, was proposed by Jiang and Wong [22]. Their global absorbing boundary condition applies to any linear hyperbolic equation with constant coefficients where the dispersion relation is known (for example, the wave equation or Klein-Gordon equation). Jiang and Wong's approach considers the group velocity, $C(k)$, of the solution at the boundaries. Remember that the flow of energy propagates at the group velocity. If we again consider the $x = 0$ boundary, any component of the solution which has a positive group velocity would obviously be a component of a reflected wave. Therefore, this boundary condition can be expressed in the following manner,

$$(10) \quad C(k)|_{x=0} = -|C(k)|_{x=0}.$$

Unfortunately, like Engquist and Majda's perfectly absorbing boundary condition (5), this absorbing boundary condition, when mapped into differential form, is non-local, due to the absolute value function, and thus a rational approximation is necessary.

To do this, Jiang and Wong use an approach similar to that utilized by Higdon [14]. First, a first order approximation is developed from the exact boundary condition (10) by assuming that the incident wave has a certain group velocity, b , which is then absorbed at the $x = 0$ boundary by

$$(11) \quad C(k)|_{x=0} + b = 0.$$

Let us consider the wave equation (3) whose dispersion relation is given in Equation (4). In this case,

$$C(k) = \frac{d\omega(k, l)}{dk} = \frac{k}{\omega}.$$

Therefore, boundary condition (11) is equivalent to the symbol $k + b\omega = 0$, or remembering the corresponding differential operators,

$$(12) \quad \left(\frac{\partial}{\partial x} - b \frac{\partial}{\partial t} \right) u|_{x=0} = 0.$$

Therefore, taking Higdon's lead [14], the canonical form of this absorbing boundary condition is

$$(13) \quad \left[\prod_{j=0}^p \left(\frac{\partial}{\partial x} - b_j \frac{\partial}{\partial t} \right) \right] u|_{x=0} = 0.$$

This is equivalent to Higdon's canonical form if $b_j = 1/\cos\alpha_j$. As before, (13) is perfectly absorbing for incident waves with group velocities b_j . The advantage of this approach is all we need to know is the dispersion relation, and we can derive the absorbing boundary conditions to any order by using the group velocity.

In [20], Higdon developed canonical radiation boundary conditions for the dispersive wave equation. Higdon showed that the performance of the boundary condition was not sensitive to the choice of parameters for the boundary condition. Further, Higdon showed that another absorbing boundary condition developed for the dispersive wave would either be equivalent to his canonical form, unstable, or not optimal in the sense the absorbing boundary condition could be modified, without increasing its order, to make it more effective. Thus, if a canonical absorbing boundary condition is found, either through using phase velocity, group velocity, or another technique, it will reduce to one ideal canonical form.

2.1.6. Other Wave Equations. In the field of Optics, Hadley considers a transparent boundary condition for beam propagation [10] [11]. The problem of interest considers the propagation of a single scalar component of the radiation field, E , which Hadley assumes to have the form

$$(14) \quad E = E_0 e^{ik_x x},$$

at the boundary where E_0 and k_x are complex. From the interior equation with diffraction being ignored, it is straightforward to show that the flux of E leaving the interior is $F(E) = \frac{\text{Re}(k_x)|E(b)|^2}{k}$, where b is the value of x at the boundary. Hadley discretizes Equation (14) as $E_{j+1}^n = E_j^n e^{ik_x \Delta x}$ where k_x is calculated from the previous $n-1$ z spatial step (z and x being orthonormal directions). This approach is similar in nature to the floating phase velocity approach used by Orlanski [34] for gravity wave propagation.

For the Helmholtz and Laplacian equations, Keller and Givoli devise non-local absorbing boundary conditions where the finite element method is used to solve the differential equations [23]. They show that the non-locality of the boundary conditions does not affect the banded structure of the finite element matrix which must be solved (analogous to a finite difference implicit scheme) and the absorbing boundary condition is exact. Unfortunately, the non-local nature of the absorbing boundary condition proposed by Keller and Givoli restricts its practical application to finite element schemes.

Higdon, building on his canonical form of Engquist and Majda's absorbing boundary conditions, has considered applications with acoustic and elastic waves in two and three dimensions [17] [18], and elastic waves in stratified media [19]. These waves are common in geophysical problems. Other than the particular details in the implementation and due to the nature of the particular problem, the underlying theory with respect to absorbing boundary conditions is the same as in Higdon's previous papers [14] [16].

2.1.7. Other Absorbing Boundary Conditions Techniques. An effective method to improve the efficiency of standard absorbing boundary conditions was developed by Mei and Fang for the solution of Maxwell's equations [31]. They call their method, "superabsorption". They consider the evolution of the coupled electrical and magnetic components of a transverse magnetic (TM) wave in two dimensions, where the components of the wave are calculated on alternative half-time steps and half a spatial step apart. By comparing the errors for the different components produced by absorbing boundary conditions for the individual components, and since the components are coupled, Mei and Fang may eliminate the common error, leading to a more accurate recalculation of the individual components. In numerical experiments, Mei and Fang show that this technique can improve absorbing boundary conditions by about an order of magnitude less reflection.

An interesting alternate approach has been considered by Van Daalen *et al.* [44]. They derive absorbing boundary conditions without assuming that solutions are available beforehand and thus without knowledge of any dispersion relation. Instead, they consider the energy transmission at the boundaries, considering continuous systems where the system is governed by a Lagrangian density, \mathcal{L} . The evolution of the system is given by applying the variation principle to the action integral (the integral of the Lagrangian density over the spatial and temporal domains). The vanishing of this variation produces a "natural boundary condition," $\frac{\partial \mathcal{L}}{\partial u_i} \varepsilon_n - \frac{\partial \mathcal{L}}{\partial u_{x_i}} n_i = 0$, where ε_n is the local flux density in the normal direction to the boundary and the second term is the partial derivative of the Lagrangian density in the normal direction. In a second paper, Broeze and Van Daalen [2] consider the two dimensional wave equation (3) as an example. Since the group velocity (i.e., the local flux density on the boundary) is 'floating' in the implementations, the approach of Van Daalen and Broeze is closely related to the 'floating phase velocity' approach with the Sommerfeld radiation boundary condition.

2.2. Stability and Well-Posedness of Absorbing Boundary Conditions. Of course, if a boundary condition is unstable or generates spurious solutions, it is useless. Issues related to stability and well-posedness of absorbing boundary conditions have been considered by a number of researchers.

The main theoretical work describing the well-posedness of initial boundary value problems has been done by Kreiss [26], Sakamoto [38], and others. The well-posedness of absorbing boundary conditions for the wave equation in particular has been considered by Trefethen and Halpern [43]. The well-posedness properties of particular absorbing boundary conditions are considered in [1] [5] [15] [17] [22] [37] by their authors.

The well-posedness theory is closely related to the stability of finite difference approximations of initial boundary value problems for hyperbolic equations. The stability criterion for hyperbolic initial boundary value problems is outlined by Gustafsson *et al.* [9], with a group velocity interpretation of their rather abstract criterion given by Trefethen [42]. Higdon considers the theory related to well-posedness of initial boundary value problems for linear first-order hyperbolic systems [15].

3. New Absorbing Boundary Conditions . In this Section, we will develop flexible absorbing boundary conditions for Schrödinger equation.

3.1. The Schrödinger Equation. The following is the one-dimensional Schrödinger equation,

$$(15) \quad i\hbar \frac{\partial \Psi}{\partial t}(x, t) = -\frac{\hbar^2}{2m} \frac{\partial^2 \Psi}{\partial x^2}(x, t) + V(x)\Psi(x, t),$$

with related dispersion relation

$$(16) \quad \hbar^2 k^2 = 2m [\omega \hbar - V],$$

where m is the mass of the particle, $V(x)$ is the potential, Ψ is the wave-function, $\hbar = h/2\pi$ where h is Planck's constant, and $i = \sqrt{-1}$. The Schrödinger equation is a fundamental equation in the field of quantum physics. It is used to describe the propagation of a quantum particle, such as an electron, in a potential background described by $V(x)$. If $V(x) = 0$, then the particle is moving in a vacuum. The square of the wave function, $|\Psi|^2$, describes the probability distribution for the position of the particle.

3.2. Previous Absorbing Boundary Conditions. A number of techniques have been considered for boundary conditions which would remove spurious reflections from artificial boundaries during the numerical solution of the one-dimensional Schrödinger equation. Kosloff and Kosloff [25] used an enlarged computational domain and then applied a damping (or penalty) function in the artificial part of the domain to decrease the amplitude of outgoing waves. Although this method can produce good results, the enlarged domain is costly, especially for extensions to higher dimensions. A related approach was considered by Neuhasuer and Baer [33], where they added a negative complex short-range potential to the potential in the asymptotic region outside the computational domain to construct nearly perfect absorbing boundary conditions.

Work by Shibata [39] and Kuska [27], which is based primarily on the work of Engquist and Majda [5] [6], has lead to one-way absorbing boundary conditions for the Schrödinger equation. Their approach is to invert Equation (16) to obtain an expression for the sign and magnitude of the wave number,

$$(17) \quad \hbar k = \sqrt{2m[\hbar\omega - V]},$$

where the positive value for the square root corresponds to waves traveling in an increasingly positive x direction, and eventually impinging on the right-hand boundary ($x = L$). To obtain the expression for waves traveling the opposite direction, simply substitute k with $-k$. A boundary condition of the form (17) is an exact absorbing boundary condition similar to Engquist and Majda's boundary condition in Equation (5). To see this, consider all waves incident on the $x = L$ boundary satisfying (17). Then there are no waves where $\hbar k = -\sqrt{2m[\hbar\omega - V]}$ at the boundary, and thus there are no left-traveling (hence reflected) waves. But due to the square root function, (17) can not be implemented directly in physical space, but rather (17) must be put in rational differential form, and thus into a finite difference form, to be implemented on the boundary.

In order to develop a differential equation to create a boundary condition transparent to waves leaving the domain, the right hand side of Equation (17) must be approximated by a rational expression. In terms of the one-dimensional Schrödinger equation, two rational expressions for the square root function have been considered

in the literature. The first was developed by Shibata [39] and has the following form:

$$(18) \quad \hbar k = \frac{\sqrt{2m\alpha_2} - \sqrt{2m\alpha_1}}{\alpha_2 - \alpha_1} [\hbar\omega - V] + \frac{\alpha_2\sqrt{2m\alpha_1} - \alpha_1\sqrt{2m\alpha_2}}{\alpha_2 - \alpha_1},$$

where α_1 and α_2 are adjustable parameters. Equation (18) is a straight line interpolation of Equation (17), which intersects the dispersion relation at two points.

A second approximation to Equation (17) was developed by Kuska [27] and has the form:

$$(19) \quad \hbar k = \hbar k_0 \frac{1 + 3z}{3 + z},$$

with $z = 2m(\hbar\omega - V)/\hbar^2 k_0^2$. His absorbing boundary condition is based on an expansion of (17) about the value $\hbar k_0$. Equation (19) is essentially an approximation to Equation (17) which intersects the square root function at only one point. Compared to Shibata's approximation (18), (19) is a higher order approximation over the length of the dispersion relation, but is limited by the single interpolation point, and is thus less flexible.

These absorbing boundary conditions developed by Shibata and Kuska are either limited in either order of effectiveness or in flexibility to absorb different energies of incident waves.

3.3. New Absorbing Boundary Condition. Here, we will consider an alternate approach to that used by Shibata and Kuska. First, we will assume that the potential is constant in time, such that $V = \{\text{finite set of constant values}\}$ or $\partial V/\partial t = 0$, and is a constant value ($V = K$) in the vicinity of the boundaries. Therefore, from the dispersion relation, Equation (17), we can calculate the group velocity,

$$(20) \quad C = \frac{\partial\omega}{\partial k} = \frac{\hbar k}{m}.$$

This gives the group velocity of a wave packet as it is evolved by the Schrödinger equation.

The following approach of using the group velocity to develop absorbing boundary conditions was first used by Jiang and Wong for hyperbolic differential equations [22]. For a wave traveling to the right within the domain and impinging on the $x = L$ boundary, the group velocity from (20) must be positive, since the energy of the wave propagates at group velocity. This implies that the energy associated with k is leaving the interior domain. A negative group velocity would mean that energy is entering the interior domain and hence is a reflected wave.

Put in mathematical form, the symbol for the boundary condition has the following form at the $x = L$ boundary,

$$(21) \quad \frac{\hbar k}{m} = \left| \frac{\hbar k}{m} \right|.$$

For the $x = 0$ boundary, simply replace k with $-k$. The pseudo-differential boundary condition that could be developed from this symbol is an exact absorbing boundary condition if satisfied on the boundary since all the group velocities on the boundary are positive (no spurious reflections off the boundary). But, like Equation (17), this boundary condition cannot be realized in physical space by differential operators due

to the absolute value function, and thus we must use an approximation to obtain an explicit rational differential form which can be applied on the boundary.

Since a single differential equation can only absorb waves of a certain group velocity, let us consider an approximation to (21) of the form of

$$(22) \quad \frac{\hbar k}{m} \equiv a,$$

on the boundary, where a is positive and real. Using the correspondence between the dual k and the partial derivative in x , we obtain the following differential operator relation from (22),

$$(23) \quad \left(i \frac{\partial}{\partial x} + \frac{ma}{\hbar} \right) \Psi = 0.$$

If this differential equation is satisfied on the boundary, then waves traveling to the right with group velocity a would be absorbed completely leading to no reflections off the boundary from that component of the numerical solution for the wave.

But in general waves are composed of more than one component with different group velocities. So, a generalization of the operator in Equation (23) is

$$(24) \quad \prod_{l=1}^p \left(i \frac{\partial}{\partial x} + \frac{ma_l}{\hbar} \right) \Psi = 0.$$

Here, the group velocity values, a_l , are real, from Equations (17) and (20), assuming $\hbar\omega \geq V$. For waves traveling to the left and impinging on the $x = 0$ boundary, a_l would be substituted with $-a_l$ in equation (24). The motivation for this generalization comes from a similar generalization that was considered by Higdon [14] which was shown to correspond to the known absorbing boundary conditions developed by Engquist and Majda [5] and others, for wave equations, as discussed in Chapter 2.

If $a_k \neq a_l$, $k \neq l$, then the effect of the differential equation (24), when applied to the boundary, would be to completely absorb p different components of the computed wave solution with p different group velocities, each being absorbed to the first order. If $a_k = a_l$, $k \neq l$, then the effect of this differential equation, when applied to the boundary, would be to completely absorb the component of the computed wave solution with group velocity a_j to the p th order. Each ma_i/\hbar can be considered as an interpolation point of the dispersion relation at the value k in Equation (16). Therefore, in (24) the ma_i/\hbar interpolates (16) at different values of k with p being the order of the interpolation. If all the group velocities a_i are the same, then (24) is essentially a series expansion of (16) to the p th order about the point ma_i/\hbar .

3.4. Comparison with Previous Work. Equation (24) is a general absorbing boundary condition from which it is possible to derive the specific absorbing boundary conditions presented by Shibata and Kuska. To see this, first consider $p = 2$. Then Equation (24) has the symbol (where we have replaced $i\partial/\partial x$ with $-k$),

$$(25) \quad \left(-k + \frac{ma_1}{\hbar} \right) \left(-k + \frac{ma_2}{\hbar} \right) = 0.$$

If we multiply out (25) and solve for $\hbar k$, then we obtain

$$(26) \quad \hbar k = \frac{2}{a_1 + a_2} (\hbar\omega - V) + \frac{ma_1 a_2}{a_1 + a_2}.$$

Here we have used Equation (16) to substitute for k^2 . Note that Equation (26) is symmetric in a_j 's. To obtain the equation for left-going waves, replace the left-hand side of Equation (26) with $-\hbar k$. Shibata's relationship in Equation (18) reduces to Equation (26) via the following substitutions,

$$\alpha_1 = \frac{ma_1^2}{2} \text{ and } \alpha_2 = \frac{ma_2^2}{2}.$$

Although Kuska states that α_1 and α_2 as used by Shibata are two "unphysical parameters" [27], we may attach meaning to them in that they are kinetic energy parameters, where the kinetic energy is propagating at group velocities a_1 and a_2 .

Now, consider $p = 3$. Then Equation (24) has the symbol

$$(27) \quad \left(-k + \frac{ma_1}{\hbar}\right) \left(-k + \frac{ma_2}{\hbar}\right) \left(-k + \frac{ma_3}{\hbar}\right) = 0,$$

where the same substitution for $i\partial/\partial x$ was used. Again, using (16) to substitute for k^2 , this simplifies to the relation

$$(28) \quad \hbar k = \frac{2mh_1(\hbar\omega - V) + h_3}{2m(\hbar\omega - V) + h_2},$$

where

$$\begin{aligned} h_1 &= m(a_1 + a_2 + a_3), \\ h_2 &= m^2 a_1 a_2 a_3 \left(\frac{1}{a_1} + \frac{1}{a_2} + \frac{1}{a_3} \right), \\ h_3 &= m^3 a_1 a_2 a_3. \end{aligned}$$

Again, to obtain the equation for left-going waves, multiply the right-hand side of Equation (28) by -1 . We may obtain Kuska's symbol for his absorbing boundary condition (19) by letting $a_1 = a_2 = a_3 = \frac{\hbar k_0}{m}$.

Therefore, Shibata's relationship for $\hbar k$ is equivalent to our second-order ($p = 2$) absorbing boundary condition and Kuska's relationship for $\hbar k$ is equivalent to a special case of our third-order ($p = 3$) boundary condition. Kuska's special case absorbing boundary condition (19) would be expected to work well if the incident wave on the boundary was composed homogeneously of only one k_0 component. This absorbing boundary condition would be expected to remove the k_0 component of the reflected wave to the third order. But, if the incident wave was composed of a number of different group velocity components, a more general absorbing boundary condition would be needed, which could be 'tuned' to remove the dominant reflected wave components. Otherwise, the components of the wave composed of wave packets traveling with different group velocities other than that associated with k_0 would be reflected to a large degree (this will be quantified in the next Section on reflection).

Considering that Kuska's absorbing boundary condition is simply the third-order form of (24) with identical a_i 's, we can derive the fourth-order absorbing boundary condition for comparison. Note that part of the motivation in the development of previous two absorbing boundary conditions was to develop a boundary condition which is first order in the boundary variable of interest, which is x in this case, and possibly of higher order in the other spatial and temporal variables. Hence, we obtain a boundary condition which is a first order differential on the incident boundary, in order to obtain an "interior-pointing" finite difference scheme. Continuing this

approach, let $p = 4$ in Equation (24), replacing the partial derivative in x with its corresponding wave vector,

$$(29) \quad 4m^2(\hbar\omega - V)^2 + 2m(-g_1\hbar k + g_2)(\hbar\omega - V) - g_3\hbar k + g_4 = 0,$$

where

$$\begin{aligned} g_1 &= m(a_1 + a_2 + a_3 + a_4), \\ g_2 &= m^2(a_1a_2 + a_1a_3 + a_1a_4 + a_2a_3 + a_2a_4 + a_3a_4), \\ g_3 &= m^3a_1a_2a_3a_4 \left(\frac{1}{a_1} + \frac{1}{a_2} + \frac{1}{a_3} + \frac{1}{a_4} \right), \\ g_4 &= m^4a_1a_2a_3a_4. \end{aligned}$$

Again, we have replaced k^2 with its lower order equivalent from Equation (16). If we let all the interpolation points be identical, $a_1 = a_2 = a_3 = a_4 = \frac{\hbar k_0}{m}$, then we obtain

$$(30) \quad \hbar k = \frac{\hbar k_0}{4} \left[\frac{z^2 + 6z + 1}{z + 1} \right],$$

where $z = 2m(\hbar\omega - V)/\hbar^2 k_0^2$. This would be the $p = 4$ absorbing boundary condition equivalent to Kuska's absorbing boundary condition.

3.5. Expression for Reflection. We can also calculate an expression for the amount of reflection we can expect off the absorbing boundary condition (24). Consider a wave impinging on the $x = L$ boundary, with a reflected component,

$$(31) \quad \Psi = e^{-i(\omega t - kx)} + r e^{-i(\omega t + kx)}.$$

In this expression for the wave, the first term is the incident wave, and the second term is the reflected wave with r as the reflection coefficient. If we apply our absorbing boundary condition (23) to this wave, we obtain

$$(32) \quad B\Psi = \left[-k + \frac{ma}{\hbar} \right] e^{-i(\omega t - kx)} + r \left[k + \frac{ma}{\hbar} \right] e^{-i(\omega t + kx)} = 0.$$

Therefore, the reflection coefficient is

$$(33) \quad R = |r| = \left| \frac{-k + \frac{ma}{\hbar}}{k + \frac{ma}{\hbar}} \right|.$$

Note that $|r|$ is always less than one. The general form of the reflection for the full absorbing boundary condition (24) is

$$(34) \quad R = \prod_{l=1}^p \left| \frac{-k + \frac{ma_l}{\hbar}}{k + \frac{ma_l}{\hbar}} \right|.$$

This expression for the reflection shows that where $ma_l/\hbar = k$, the absorbing boundary condition (24) is perfectly absorbing since $R = 0$. Otherwise, $|r| < 1$ and all the incident components of the wave are reduced in amplitude in the reflected wave, implying absorption of the incident wave. To minimize the reflection produced by the absorbing boundary condition, we can do two things. Since $|r|$ is less than one, the larger the value of p in (34), the smaller the value of the reflection. Hence, we seek a higher order absorbing boundary condition, where feasible, to minimize the reflection. Also, where the incident wave is composed of several wave packets with different group velocities, choosing a_l to coincide with the incident group velocities will decrease the value of the reflection given by (34).

3.6. Well-Posedness of the New Absorbing Boundary Condition. Of course, it is also very important to show that these boundary conditions given by Equation (24) generate well-posed initial boundary value problems, when coupled with the Schrödinger equation. A well-posed problem is one that does not admit either solutions with exponentially growing amplitudes anywhere in the domain, or spurious solutions generated from the boundary. We are limited in how much we can determine regarding the well-posedness of absorbing boundary conditions for the Schrödinger equation, since there is no theoretical proof, to our knowledge, of the well-posedness for the Schrödinger equation. In the absence of any formal theory, we will adapt the well-posedness theory that has been developed for the wave equation. We must keep in mind that this may, or may not, be a valid assumption, and hence our proof will proceed with the assumption that it is a valid approach.

The Kreiss condition [26] for wave equations states that for well-posedness, that the problem must i) not admit any eigenvalues, and ii) that there are no generalized eigenvalues. Eigenvalues are those complex values s that simultaneously satisfy both the dispersion relation of the interior differential equation and the symbol of the boundary condition, such that $\text{Re}(s) > 0$. If such eigenvalues exist, then the initial boundary value problem admits a normal mode e^{st} . If eigenvalues are admitted by the boundary condition, then the solution on the boundary will grow unboundedly, and hence be unstable. Generalized eigenvalues are complex values s that also satisfy the dispersion relation and the symbol of the boundary condition, but where $\text{Re}(s) = 0$ and the group velocity of the normal mode is ≥ 0 (≤ 0) on the left-hand (right-hand) boundary. If there are any generalized eigenvalues, then the boundary condition will admit a spurious traveling wave solution which will propagate energy into the interior domain.

Following the example worked out by Engquist and Majda [5] for both constant coefficient and variable coefficient wave equations, we use the general algebraic normal mode analysis for checking well-posedness, specialized for the Schrödinger equation:

PROPOSITION 3.1. *The initial boundary value problem for the Schrödinger equation is well-posed if there are no solutions to the frozen coefficient half-space problems of the form*

$$(35) \quad \tilde{\Psi}(s) = e^{-st - \sqrt{\frac{2m}{\hbar^2}[i\hbar s + V]}x},$$

with $\text{Re } s \geq 0$ (where s is complex). Here the half-space we are considering is $x \geq 0$ with the boundary at $x = 0$. A solution where $\text{Re } s > 0$ would be an eigenvalue, or a solution where $\text{Re } s = 0$ would be generalized eigenvalue. Note that the dispersion relation for the interior solutions has been substituted for the wave number in (35). The solutions would have to satisfy

$$(36) \quad i\hbar \frac{\partial \tilde{\Psi}}{\partial t}(s) = -\frac{\hbar^2}{2m} \frac{\partial^2 \tilde{\Psi}(s)}{\partial x^2} + V \tilde{\Psi}(s),$$

and

$$(37) \quad \prod_{l=1}^p \left(i \frac{\partial}{\partial x} - \frac{ma_l}{\hbar} \right) \tilde{\Psi}(s) = 0.$$

Specifically, the criterion corresponds to waves impinging on the left-hand boundary, but the result holds equally for the right-hand boundary. Applying the boundary

condition (37), with $p = 1$, to $\tilde{\Psi}$ yields the following result,

$$(38) \quad -i\sqrt{\frac{2m}{\hbar^2}[i\hbar s + V]} - \frac{ma_1}{\hbar} = 0.$$

Taking the second term to the right hand side, and squaring both sides, leads to the following relation,

$$(39) \quad s = \frac{i}{\hbar} \left(\frac{ma_1^2}{2} + V \right).$$

From (39), it is obvious that

$$(40) \quad \text{Re } s = 0,$$

since s is wholly imaginary. This implies that there are no eigenvalues. Also, since the boundary condition is constructed such that the group velocity is ≤ 0 (≥ 0) on the left-hand (right-hand) boundary, there are also no generalized eigenvalues which will propagate waves into the interior. But there is a generalized eigenvalue with zero group velocity which remains on the boundary. Therefore, if there are any instabilities which might be admitted by the generalized eigenvalue of the absorbing boundary condition, they would not propagate into the interior of the solution, and thus they will not affect the interior solution. Therefore, the boundary condition is well-posed with the except of the zero group velocity generalized eigenvalue for $p = 1$. To see that the boundary condition is also well-posed for $p > 1$, consider the product form of the boundary condition (37). Since we did not specify any particular value for a_1 , it is obvious that if there were eigenvalues or generalized eigenvalues with non-zero group velocities that violated the above criterion, they would have appeared in the analysis for $p = 1$. Since they did not, the results hold for all p and a_i , and the boundary condition is well posed for all orders of (24). Recall that this conclusion is tempered by the assumption that the initial boundary value problem well-posedness theory developed for the wave equation can applied to the Schrödinger equation.

3.7. Higher Dimensions. It is straight-forward to extend the general absorbing boundary condition (24) to two or three dimensions. Consider the Schrödinger equation in two dimensions,

$$(41) \quad i\hbar \frac{\partial \Psi(x, y, t)}{\partial t} = -\frac{\hbar^2}{2m} \left(\frac{\partial^2 \Psi(x, y, t)}{\partial x^2} + \frac{\partial^2 \Psi(x, y, t)}{\partial y^2} \right) + V(x, y)\Psi(x, y, t),$$

where m , $V(x, y)$, and $\Psi(x, y, t)$ are defined as before. The interior numerical solution for the two dimensional Schrödinger equation is given by Galbraith *et al.* [7]. Kuska developed a two dimensional version of his boundary condition as a straightforward extension of his one dimensional version (19) [27].

Following essentially the same procedure as that used to derive (24), consider a two dimensional plane wave of the form

$$(42) \quad \Psi(x, t) = e^{-i(\omega t - k_x x - k_y y)},$$

where ω is the frequency of the wave and k_x and k_y are the wave vectors in the x and y directions, respectively. Equivalently, $k_x = k \cos \phi$ and $k_y = k \sin \phi$ where ϕ is the angle of the direction of k measured from the normal (pointing away from

the interior) of the $x = a$ boundary (a can be 0 or L). Then we have the following dispersion relation

$$(43) \quad \hbar^2 k_x^2 + \hbar^2 k_y^2 = 2m [\omega \hbar - V],$$

assuming that the potential V is a constant in the neighbourhood of the boundaries. This gives us the following group velocities,

$$(44) \quad (C_x, C_y) = \left(\frac{\partial \omega}{\partial k_x}, \frac{\partial \omega}{\partial k_y} \right) = \left(\frac{\hbar k_x}{m}, \frac{\hbar k_y}{m} \right).$$

Therefore, on the $x = L$ boundary, the two dimensional version of Equation (22) is, using the same argument as in Section 3.3,

$$(45) \quad \frac{\hbar k_x}{m} \equiv a_x,$$

where a_x is the x component of a two dimensional group velocity such that $a_x = a \cos \theta$. The angle is the direction of group velocity measured from the normal of the $x = L$ boundary, as ϕ above. Since the corresponding differential operator to k_x is $-i\partial/\partial x$, our general absorbing boundary condition in two dimensions becomes

$$(46) \quad \prod_{l=1}^p \left(i \frac{\partial}{\partial x} + \frac{ma_l \cos \theta_l}{\hbar} \right) \Psi = 0.$$

Actually, $\cos \theta_l$ can be absorbed by a_l leaving a_l as the only necessary parameter. Again, for waves traveling to the left and impinging on the $x = 0$ boundary, a_l would simply be substituted by $-a_l$ in equation (46).

As before, we can derive the expected reflection produced by the two-dimensional absorbing boundary condition. If we consider an incident wave of the form

$$(47) \quad \Psi = e^{-i(\omega t - k \cos \phi x - k \sin \phi y)} + r e^{-i(\omega t + k \cos \phi x - k \sin \phi y)},$$

where r is the amplitude of the reflected component, then absorbing boundary condition (46) would generate the following reflection coefficient.

$$(48) \quad R = \prod_{l=1}^p \left| \frac{-k \cos \phi + \frac{ma_l \cos \theta_l}{\hbar}}{k \cos \phi + \frac{ma_l \cos \theta_l}{\hbar}} \right|.$$

We would choose $\cos \theta_l$ and a_l to minimize the reflection coefficient.

Let us consider a practical implementation of this two dimensional absorbing boundary condition with $p = 3$. Then, in wave vector format, Equation (46) takes the following form

$$(49) \quad \left(-k_x + \frac{ma_{x1}}{\hbar} \right) \left(-k_x + \frac{ma_{x2}}{\hbar} \right) \left(-k_x + \frac{ma_{x3}}{\hbar} \right) = 0.$$

This simplifies to the relation, with the substitution of terms of k_x^2 with (43),

$$(50) \quad \hbar k_x = \frac{2m\tilde{h}_1(\hbar\omega - V) - \hbar^2\tilde{h}_1k_y^2 + \tilde{h}_3}{2m(\hbar\omega - V) - \hbar^2k_y^2 + \tilde{h}_2},$$

where

$$\begin{aligned}\tilde{h}_1 &= m(a_{x1} + a_{x2} + a_{x3}), \\ \tilde{h}_2 &= m^2 a_{x1} a_{x2} a_{x3} \left(\frac{1}{a_{x1}} + \frac{1}{a_{x2}} + \frac{1}{a_{x3}} \right), \\ \tilde{h}_3 &= m^3 a_{x1} a_{x2} a_{x3}.\end{aligned}$$

In explicit differential form, where we have substituted for the duals in the symbol (50) with their respective differential operators, this absorbing boundary condition evaluated at the $x = L$ boundary would have the form

$$(51) \quad \left[-\hbar^3 i \frac{\partial^3 \Psi}{\partial x \partial y^2} + 2m\hbar^2 \frac{\partial^2 \Psi}{\partial t \partial x} - \hbar^2 \tilde{h}_1 \frac{\partial^2 \Psi}{\partial y^2} - 2m\hbar \tilde{h}_1 i \frac{\partial \Psi}{\partial t} + \hbar i (2mV - \tilde{h}_2) \frac{\partial \Psi}{\partial x} + (2m\tilde{h}_1 V - \tilde{h}_3) \Psi \right] \Big|_{x=L} = 0.$$

If $a_{xj} = \hbar k_{0x}/m$, then we recover the absorbing boundary condition given by Kuska in his equation (11), with k_{0x} being defined as the x component of the initial wave vector k_0 [27].

4. Numerical Tests of Absorbing Boundary Conditions . In this Section, we will a finite-difference scheme to test the effectiveness of various orders of the general absorbing boundary condition (24). This scheme will used with several initial distributions of i) a single Gaussian distribution modulating a traveling plane wave, ii) the sum of two Gaussian distributions modulating two waves traveling at different initial group velocities, and iii) a pseudo-delta function approximated by a Gaussian distribution with small initial spread modulating a single plane wave. The amount of reflection generated by the absorbing boundary conditions will be compared at the different orders to determine their relative effectiveness.

4.1. Schrödinger Equation Implicit Interior Scheme. For the numerical results, an implicit finite-difference interior scheme will be used to numerically solve the Schrödinger equation. The spatial domain of the numerical solution of Equation (15) is $x = x_j = j\epsilon$, with $j \in [0, \mathcal{J}]$, where ϵ is the spatial mesh width. Therefore, the left-most boundary is $x = 0$ and the right-most boundary is $x = \mathcal{J}\epsilon = L$. Similarly, the time variable has the following range, $t = t_n = n\delta$, with $n = 0, 1, 2, \dots, N$. $\Psi(x_j, T = N\delta)$ are the last calculated wave-function values. We will discuss later how to choose N . Along the same lines, the discretization of the wave function is $\Psi_j^n = \Psi(x_j, t_n)$.

We will use following implicit scheme [8],

$$(52) \quad \begin{aligned} \Psi_{j+1}^{n+1} + \left(-2 + \frac{4im}{\hbar\lambda} - \frac{2m\epsilon^2 V_j}{\hbar^2} \right) \Psi_j^{n+1} + \Psi_{j-1}^{n+1} = \\ -\Psi_{j+1}^n + \left(2 + \frac{4im}{\hbar\lambda} + \frac{2m\epsilon^2 V_j}{\hbar^2} \right) \Psi_j^n - \Psi_{j-1}^n, \end{aligned}$$

where $\lambda = \delta/\epsilon^2$. The discretization V_j implies the value $V(x_j)$. The implicit scheme is based on the calculation of the next time step of the integration using only the previous time step. This scheme preserves the unitarity of the wave-function, as well as meet the von Neumann test requirement [12,p.102].

4.2. Numerical Schemes for the Absorbing Boundary Condition. To numerically implement the absorbing boundary conditions, we need to discretize the differential operators to produce finite difference schemes. We will consider a number of orders (p) of the general absorbing boundary condition (24).

4.2.1. The $p = 2$ Absorbing Boundary Condition. This boundary condition is based on Equation (26). This boundary condition is equivalent to the absorbing boundary condition presented by Shibata [39] in Equation (18). Translated into explicit differential form, the absorbing boundary condition becomes

$$(53) \quad \pm i\hbar \Psi_x - i\hbar c_1 \Psi_t + (c_1 V(x) - c_2) \Psi = 0,$$

where

$$(54) \quad c_1 = \frac{2}{a_1 + a_2}, \quad c_2 = \frac{ma_1 a_2}{a_1 + a_2}.$$

The positive sign on the first term refers the boundary condition applied to the $x = 0$ boundary and the negative sign refers to the $x = L$ boundary.

The following finite-difference discretizations [27] will be used for the differential operators in (53).

$$(55) \quad \Psi \approx \frac{(Z + I)}{2} \frac{(J^\pm + I)}{2} \Psi_j^n,$$

$$(56) \quad \Psi_x \approx \pm \frac{(Z + I)}{2} \frac{(J^\pm - I)}{\epsilon} \Psi_j^n,$$

$$(57) \quad \Psi_t \approx \frac{(J^\pm + I)}{2} \frac{(Z - I)}{\delta} \Psi_j^n,$$

where the top sign of a double-signed term refers to the $x = 0$ boundary condition and the bottom sign refers to the $x = L$ boundary condition (from the negative and positive values for wave vector k , denoting left and right-traveling waves, respectively). This abbreviation convention will be used throughout. In the above, the following shift operators were used, $J\Psi_j^n = \Psi_{j+1}^n$, $I\Psi_j^n = \Psi_j^n$, $J^-\Psi_j^n = \Psi_{j-1}^n$. Similar shift operators will also be used for time operations, $Z\Psi_j^n = \Psi_j^{n+1}$, $Z^-\Psi_j^n = \Psi_j^{n-1}$.

Using these discretizations in (53) yields the following $p = 2$ absorbing boundary condition,

$$(58) \quad \begin{aligned} & \left(\frac{i\hbar}{2\epsilon} - \frac{i\hbar c_1}{2\delta} + \frac{(c_1 V_{(0,\mathcal{J})} - c_2)}{4} \right) \Psi_{(1,\mathcal{J}-1)}^{n+1} \\ & + \left(-\frac{i\hbar}{2\epsilon} - \frac{i\hbar c_1}{2\delta} + \frac{(c_1 V_{(0,\mathcal{J})} - c_2)}{4} \right) \Psi_{(0,\mathcal{J})}^{n+1} \\ & = \left(-\frac{i\hbar}{2\epsilon} - \frac{i\hbar c_1}{2\delta} - \frac{(c_1 V_{(0,\mathcal{J})} - c_2)}{4} \right) \Psi_{(1,\mathcal{J}-1)}^n \\ & + \left(\frac{i\hbar}{2\epsilon} - \frac{i\hbar c_1}{2\delta} - \frac{(c_1 V_{(0,\mathcal{J})} - c_2)}{4} \right) \Psi_{(0,\mathcal{J})}^n. \end{aligned}$$

The abbreviation for the wave function, $\Psi_{(1,\mathcal{J}-1)}^{n+1}$, denotes that the discrete scheme uses the value Ψ_1^{n+1} on the $x = 0$ boundary, and $\Psi_{\mathcal{J}-1}^{n+1}$ on the $x = L$ boundary.

4.2.2. The $p = 3$ Absorbing Boundary Condition. This boundary condition is based on Equation (28). A special case of this boundary condition would yield the absorbing boundary condition considered by Kusk [27] in Equation (19). Rewritten in explicit differential form, Equation (28) has the form

$$(59) \quad \pm i\hbar \left(\frac{h_2}{2m} - V(x) \right) \Psi_x \mp \hbar^2 \Psi_{tx} - i\hbar h_1 \Psi_t - \left(\frac{h_3}{2m} - h_1 V(x) \right) \Psi = 0,$$

where h_i are defined in the previous Section.

The finite difference discretizations given in Equations (55) to (57), along with the following discretization [27], will be used for the differential operators in (59).

$$(60) \quad \Psi_{tx} \approx \pm \frac{(Z - I)(J^\pm - I)}{\delta \epsilon} \Psi_j^n.$$

These discretizations applied to Equation (59) yield the following $p = 3$ absorbing boundary condition,

$$(61) \quad \begin{aligned} & \left(\frac{a}{2\epsilon} - \frac{b}{\delta\epsilon} - \frac{c}{2\delta} - \frac{d}{4} \right) \Psi_{(1,\mathcal{J}-1)}^{n+1} + \left(-\frac{a}{2\epsilon} + \frac{b}{\delta\epsilon} - \frac{c}{2\delta} - \frac{d}{4} \right) \Psi_{(0,\mathcal{J})}^{n+1} \\ & = \left(-\frac{a}{2\epsilon} - \frac{b}{\delta\epsilon} - \frac{c}{2\delta} + \frac{d}{4} \right) \Psi_{(1,\mathcal{J}-1)}^n + \left(\frac{a}{2\epsilon} + \frac{b}{\delta\epsilon} - \frac{c}{2\delta} + \frac{d}{4} \right) \Psi_{(0,\mathcal{J})}^n, \end{aligned}$$

where $a = i\hbar \left(\frac{h_2}{2m} - V_{(0,\mathcal{J})} \right)$, $b = \hbar^2$, $c = i\hbar h_1$, $d = \left(\frac{h_3}{2m} - h_1 V_{(0,\mathcal{J})} \right)$.

4.2.3. The $p = 4$ Absorbing Boundary Condition. Equation (29) for $p = 4$ leads to the following differential absorbing boundary condition,

$$(62) \quad p_1 \Psi_{tt} \pm p_2 \Psi_{tx} + p_3 \Psi_t \pm p_4 \Psi_x + p_5 \Psi = 0,$$

where $p_1 = -4m^2 \hbar^2$, $p_2 = 2mg_1 \hbar^2$, $p_3 = 2mi\hbar g_2 - 8m^2 i\hbar V_{(0,\mathcal{J})}$, $p_4 = 2mi\hbar g_1 V_{(0,\mathcal{J})} - i\hbar g_3$, $p_5 = 4m^2 (V_{(0,\mathcal{J})})^2 - 2mg_2 V_{(0,\mathcal{J})} + g_4$, where g_i are defined as before, in Section 3. To discretize this differential boundary condition, we will use

$$(63) \quad \Psi_{tt} \approx -\frac{(Z^- - I)(Z - I)}{\delta^2} \Psi_j^n.$$

along with the discretizations given in Equations (55) to (57) and Equation (60). The result of these discretizations in Equation (62) yields the following $p = 4$ absorbing boundary condition.

$$(64) \quad \begin{aligned} & \left(\frac{p_2}{\delta\epsilon} + \frac{p_3}{2\delta} + \frac{p_4}{2\epsilon} + \frac{p_5}{4} \right) \Psi_{(1,\mathcal{J}-1)}^{n+1} + \left(\frac{p_1}{\delta^2} - \frac{p_2}{\delta\epsilon} + \frac{p_3}{2\delta} - \frac{p_4}{2\epsilon} + \frac{p_5}{4} \right) \Psi_{(0,\mathcal{J})}^{n+1} \\ & = \left(\frac{p_2}{\delta\epsilon} + \frac{p_3}{2\delta} - \frac{p_4}{2\epsilon} - \frac{p_5}{4} \right) \Psi_{(1,\mathcal{J}-1)}^n + \left(2\frac{p_1}{\delta^2} - \frac{p_2}{\delta\epsilon} + \frac{p_3}{2\delta} + \frac{p_4}{2\epsilon} - \frac{p_5}{4} \right) \Psi_{(0,\mathcal{J})}^n \\ & + \left(-\frac{p_1}{\delta^2} \right) \Psi_{(0,\mathcal{J})}^{n-1} \end{aligned}$$

Note that two previous time levels are needed to calculate the subsequent time level in (64).

4.3. Numerical Results. The initial conditions used for all numerical calculations is a Gaussian distribution (either singularly or in combinations),

$$(65) \quad \Psi_j^0 = e^{-(x_j - \xi)^2 / 2\sigma_0^2} e^{iK_0 x_j}.$$

In all the following calculation results, unless otherwise stated, $m = 0.5$ and $\hbar = 1$. Also, the potential $V(x)$ will be set to zero for all calculations.

What does this choice for initial conditions tell us about the applicability of the boundary conditions with respect to completely general initial conditions? We note that any general initial conditions can be expressed in terms of a Fourier series, and a single Fourier mode is essentially a plane wave. Therefore, since the Gaussian distribution's carrier wave is a plane wave, if the boundary conditions are well behaved for various frequencies of plane waves in our examples, then the boundary condition would be expected to be well-behaved for any arbitrary choice of initial conditions whose Fourier modes are dominant at the same frequencies.

4.3.1. Tests of the Reflection Properties of the General Absorbing Boundary Condition. We will compare the relative properties, in terms of reflection, of different orders of the general absorbing boundary condition (24, with respect to each other and with respect to the exact solution. Also, the effectiveness of the more general form of (24) will be considered in comparison with the published absorbing boundary conditions of Shibata [39] and Kusk [27].

The reflection ratio r at t_n was calculated as [27]

$$(66) \quad r = \frac{\sum_{j=0}^{\mathcal{J}} |\Psi_j^n|^2}{\sum_{j=0}^{\mathcal{J}} |\Psi_j^0|^2}$$

This r is similar to the reflection coefficient $|r|$ in (33). Here, r is the ratio of the integration of the squared amplitude of the reflected wave-function over the initial wave-function (essentially, the ratio of the reflected wave with respect to the initial wave). Since our wave-functions are discrete, the integration is a summation over the domain. When the wave is completely reflected then $r = 1$, whereas if the wave is completely absorbed, then $r = 0$, after the initial wave has passed through the absorbing boundary condition. To compare the different schemes, we will plot the reflection ratio as a function of time. This method of comparison is most useful when only one wave is passing through a boundary at a time. When no waves are passing through either boundary and any traveling waves are presently only in the interior of the domain, then the reflection ratio as a function of time is a plateau whose value measures the total wave amplitude remaining in the interior of the domain. Waves smoothly passing through a boundary are represented by a smoothly decreasing reflection ratio as a function of time. As the waves present in the interior domain are diminished by passing through the absorbing boundary conditions, r eventually goes to zero. The reflection ratio values that we are primarily interested in are the midpoints of the first plateau, when the Gaussian distribution has passed through the $x = L$ boundary and any waves reflected are still in the interior of the domain and have not yet reached the $x = 0$ boundary. Obviously, for more arbitrary wave solutions, this method of comparison would not be adequate on small domains, since we would not be able to tell when the particular waves we are interested in are passing through the boundaries.

No.	Implicit Scheme	K_0	time	r
1	$p = 2, \mathcal{J} = 512$	5.0	1.5	2.024×10^{-2}
2	$p = 2, \mathcal{J} = 1024$	5.0	1.5	2.007×10^{-2}
3	$p = 3, \mathcal{J} = 512$	5.0	1.5	4.193×10^{-6}
4	$p = 3, \mathcal{J} = 1024$	5.0	1.5	3.750×10^{-6}
5	$p = 4, \mathcal{J} = 512$	5.0	1.5	1.325×10^{-5}
6	$p = 4, \mathcal{J} = 1024$	5.0	1.5	3.618×10^{-6}
7	$p = 2, \mathcal{J} = 512$	15.0	0.3	2.250×10^{-2}
8	$p = 2, \mathcal{J} = 1024$	15.0	0.3	2.090×10^{-2}
9	$p = 3, \mathcal{J} = 512$	15.0	0.3	2.935×10^{-5}
10	$p = 3, \mathcal{J} = 1024$	15.0	0.3	1.829×10^{-6}
11	$p = 4, \mathcal{J} = 512$	15.0	0.3	1.297×10^{-4}
12	$p = 4, \mathcal{J} = 1024$	15.0	0.3	3.073×10^{-5}
13	$p = 2, \mathcal{J} = 512$	30.0	0.15	2.945×10^{-2}
14	$p = 2, \mathcal{J} = 1024$	30.0	0.15	2.254×10^{-2}
15	$p = 3, \mathcal{J} = 512$	30.0	0.15	4.754×10^{-4}
16	$p = 3, \mathcal{J} = 1024$	30.0	0.15	2.907×10^{-5}
17	$p = 4, \mathcal{J} = 512$	30.0	0.15	9.370×10^{-4}
18	$p = 4, \mathcal{J} = 1024$	30.0	0.15	1.765×10^{-4}

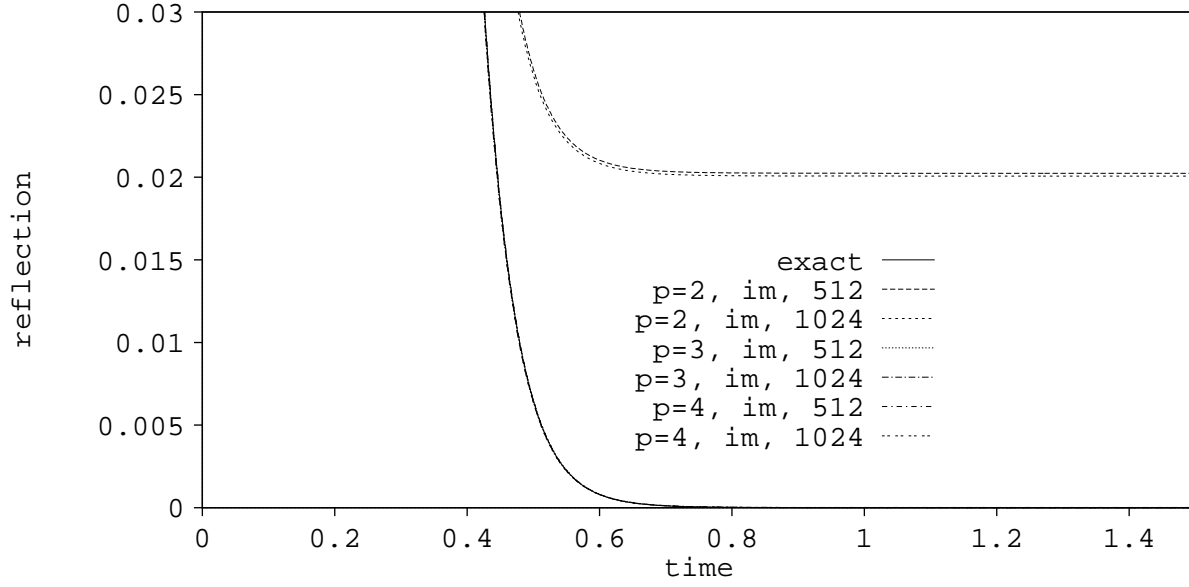
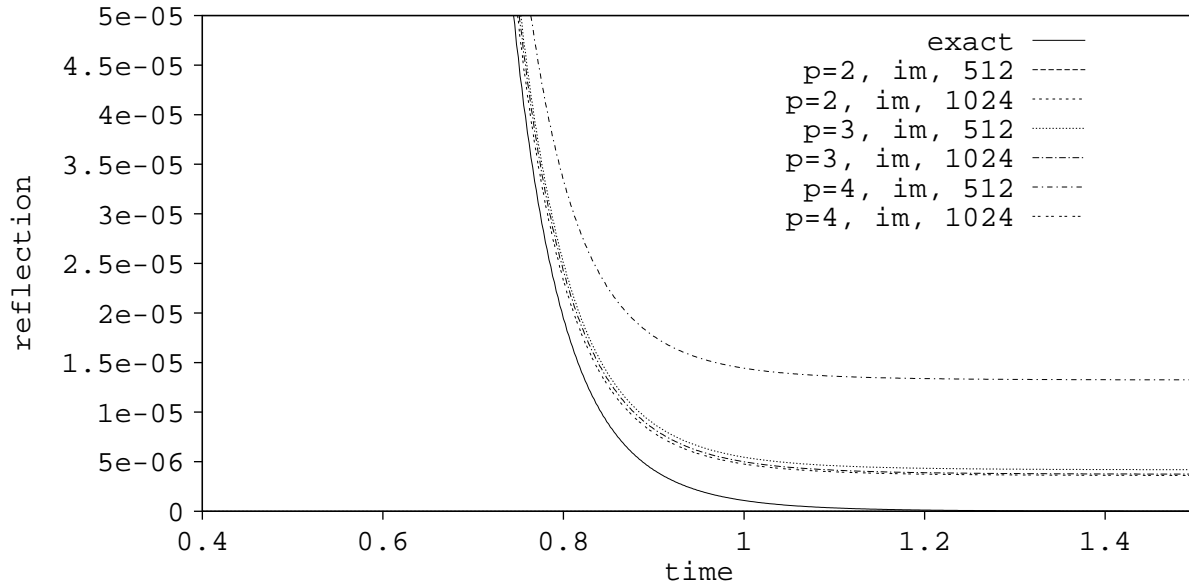
TABLE 1

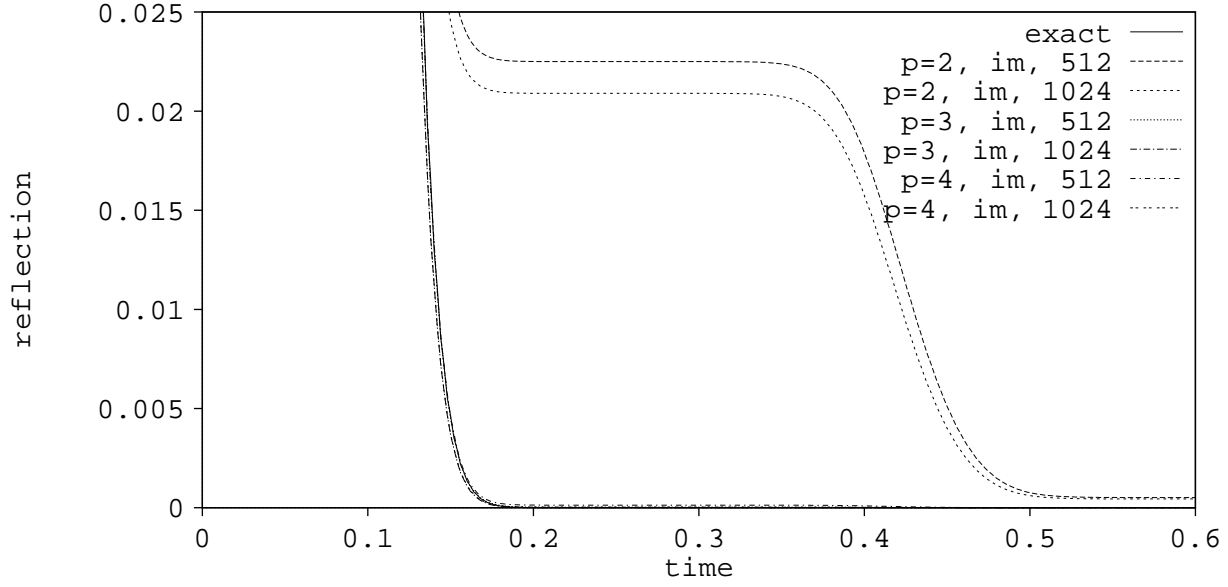
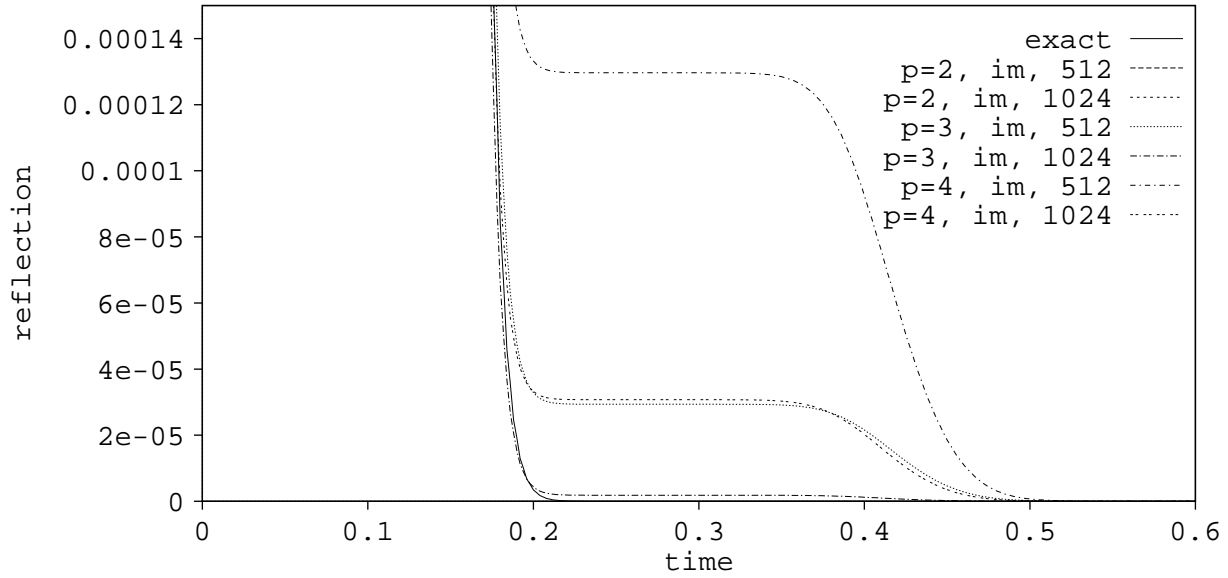
Comparison of Reflection Ratios vs. Different Schemes for Single Gaussian.

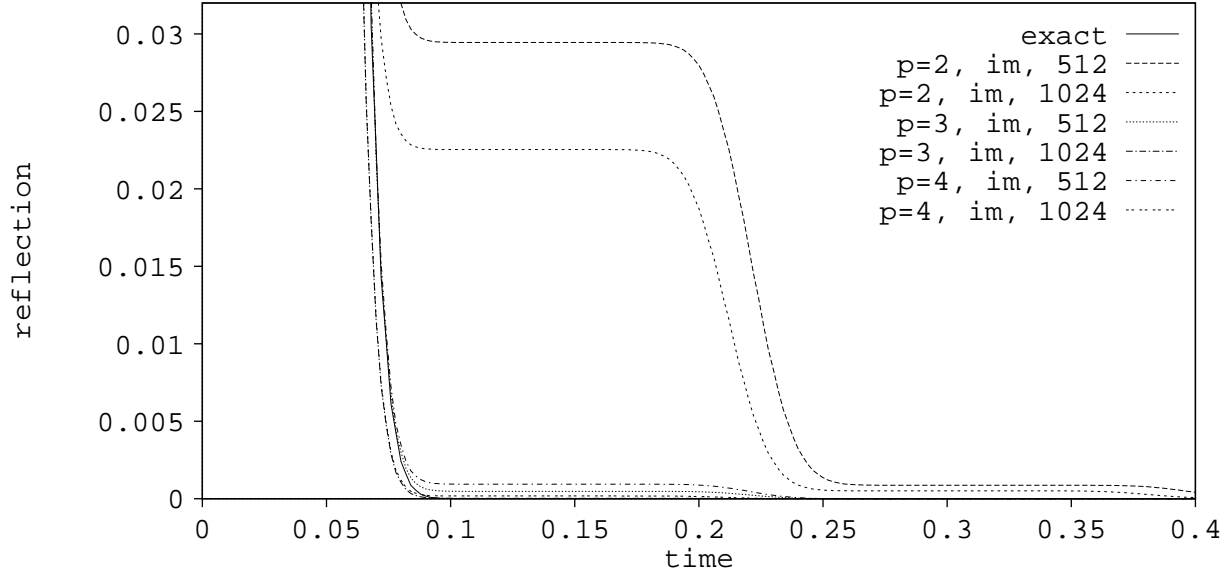
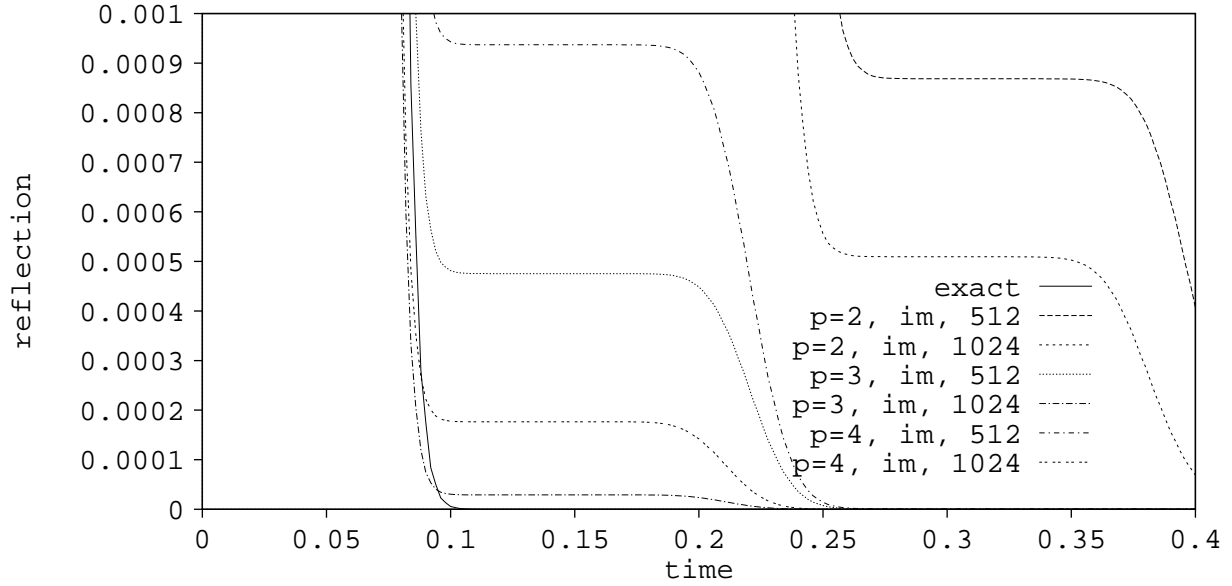
4.3.2. Single Gaussian Distribution. The first set of comparisons will use an initial distribution of a single Gaussian distribution as given by Equation (65). Figures 1 to 6 show plots of reflection ratio as a function of time for $K_0 = 5, 15$, and 30 , with $L = 10, \sigma_0 = L/10$, and $\xi = 3L/4$ (with an exception for $K_0 = 5$ where the range of x used was $[-20, 10]$, so that any reflection from the $x = 0$ boundary do not affect the results). For all computations, $\delta = 0.0001$ and $a_i = \hbar K_0/m$ for the absorbing boundary conditions. The various orders of the general absorbing boundary condition and different spatial sizes of the grid are compared. Listed on the plots are the value of p of the boundary condition and the value of \mathcal{J} from which $\epsilon = L/\mathcal{J}$ is determinable. The ‘im’ implies that the scheme used is an implicit scheme. The relative values of reflection ratios for the different schemes are shown in Table 1 at various time slices, chosen to coincide with the midpoints of the reflection ratio plateaus in Figures 1 to 6.

It is obvious from the values in Table 1 and from the plots in Figures 1 to 6 that the reflection ratio is lower for the higher order absorbing boundary conditions. It is a bit unexpected that the $p = 3$ absorbing boundary condition performed better than the $p = 4$ which we would expect to have a lower reflection ratio value as predicted by Equation (34). This will be discussed later. Also, the smaller the grid spacing ϵ , the less reflection produced by the absorbing boundary condition.

Now, assume that we use the same Gaussian distribution calculation, again, using the implicit interior schemes, but vary the interpolated group velocities of the absorbing boundary condition for $p = 3$ and $p = 4$ as follows: $a_i = (1 + \zeta) \frac{\hbar K_0}{m}$, where ζ is the variation of group velocity. The rationale for this type of calculation is two-fold. First, as the Gaussian distribution evolves via the Schrödinger equation, the distribution in momentum space spreads [8]. Also, a calculation of the group velocity at

FIG. 1. *Reflection Ratio as a Function of Time for $K_0 = 5.0$.*FIG. 2. *Reflection Ratio as a Function of Time for $K_0 = 5.0$ - close-up.*

FIG. 3. *Reflection Ratio as a Function of Time for $K_0 = 15.0$.*FIG. 4. *Reflection Ratio as a Function of Time for $K_0 = 15.0$ - close-up.*

FIG. 5. *Reflection Ratio as a Function of Time for $K_0 = 30.0$.*FIG. 6. *Reflection Ratio as a Function of Time for $K_0 = 30.0$ - close-up.*

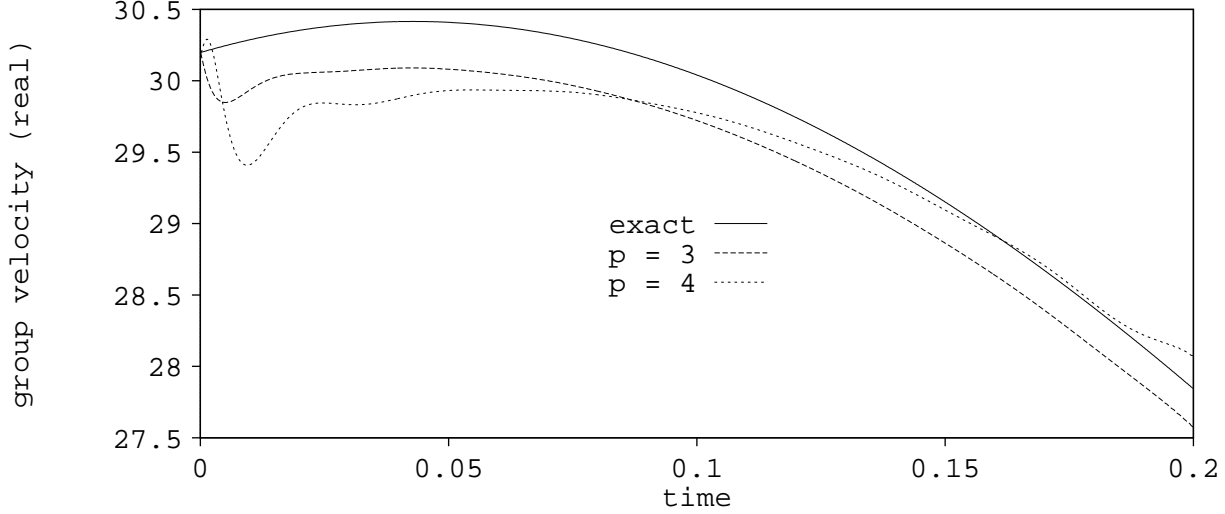


FIG. 7. Measured Group Velocity as a function of time at the $x = L$ boundary for $K_0 = 15.0$ (real component).

the $x = L$ boundary as the single Gaussian distribution passes through boundary will reveal that the real component of the group velocity of the distribution increases and then decreases after the peak of the distribution has passed through the boundary, as we can see in Figure 7, whereas the imaginary component simply decreases as in Figure 8. Hence, we would not expect the initial value of the group velocity to give the best results for the absorbing boundary condition. Also, each order of the general absorbing boundary condition will interpolate the exact dispersion relation for the Schrödinger equation differently. Hence the properties of each order of the absorbing boundary condition will be different according to how the initial distribution evolves with respect to the form of the interpolation.

But since the higher order absorbing boundary conditions have multiple degrees of freedom, we will use a simple one degree of freedom test of the properties of the $p = 3$ and $p = 4$ absorbing boundary conditions. Using ζ as the variable and the values of a_i shown above, then we obtain the results in Figure 9. Obviously, the higher values of a_i allow the $p = 3$ absorbing boundary condition to reduce reflection ratio, reaching its optimal performance at $a_i \approx 1.39\hbar K_0/m$. For even higher values of a_i , the $p = 4$ absorbing boundary condition improves its absorption properties to the point where its reflection ratio is only a few times higher than the optimal value for the $p = 3$ absorbing boundary condition.

4.3.3. Double Gaussian Distribution. The next series of comparisons will use an initial distribution composed of two Gaussian distributions with different initial group velocities. Initially, the distribution has the form

$$(67) \quad \Psi_j^0 = \frac{e^{-(x_j - \xi)^2 / 2\sigma_0^2} e^{iK_0 x_j} + e^{-(x_j - \xi)^2 / 2\sigma_0^2} e^{iK_1 x_j}}{\sqrt{2}}.$$

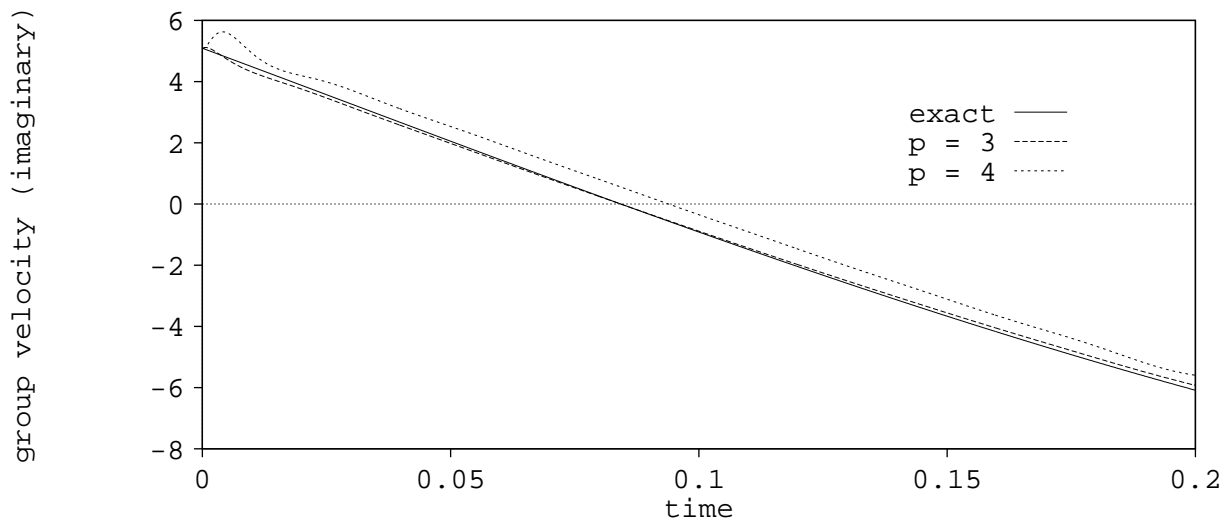
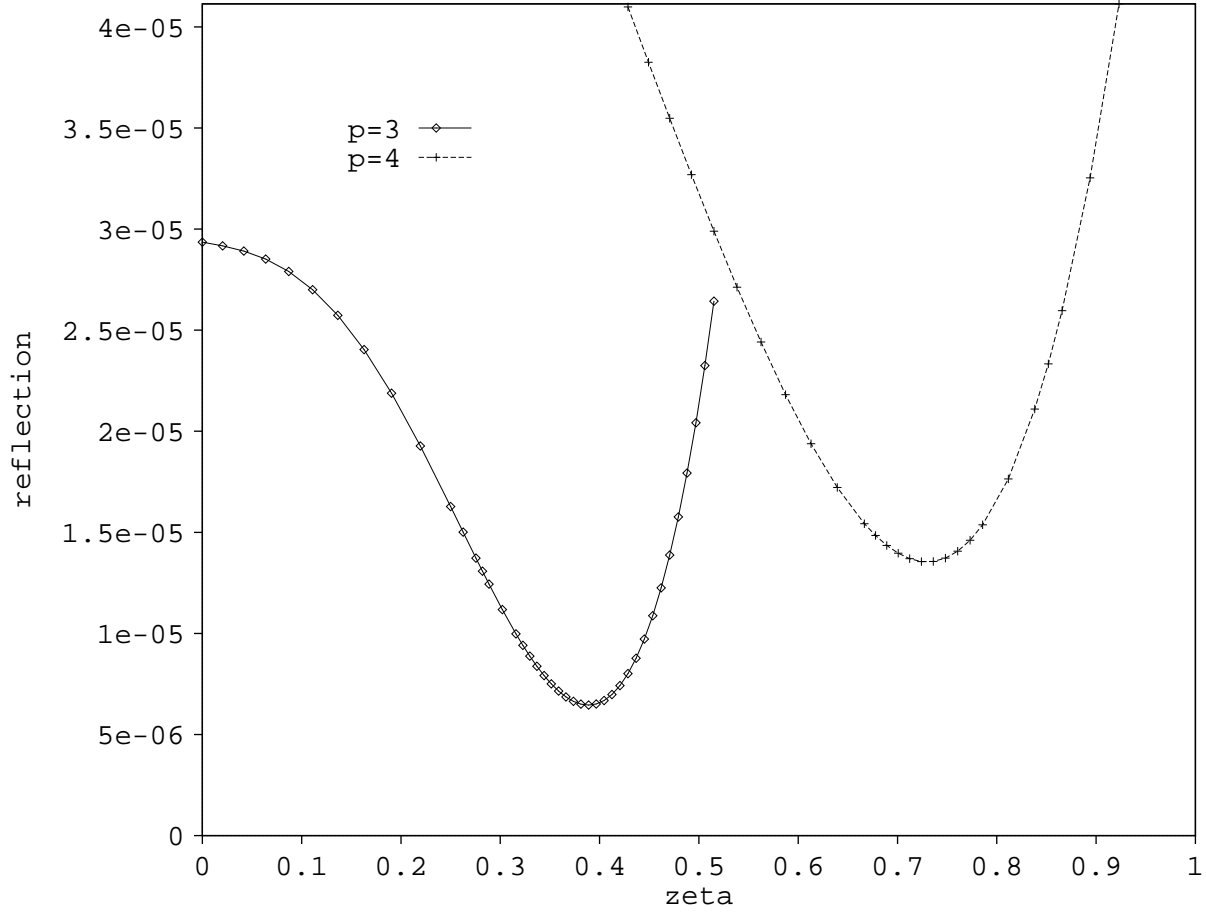


FIG. 8. Measured Group Velocity as a function of time at the $x = L$ boundary for $K_0 = 15.0$ (imaginary component).

For our calculations, $K_0 = 25$, $K_1 = 5$, $\epsilon = 10/512$, $\delta = 0.0001$, $\sigma_0 = 1$, and $\xi = 7.5$. The calculation was carried out using the implicit solution for the interior of the domain, and the $p = 3$ and $p = 4$ absorbing boundary conditions. The key of the plots contains the value of p , and a series of ones and zeros for the values of a_1, a_2, a_3 (and a_4 if the scheme is $p = 4$), respectively. A ‘one’ indicates that the corresponding value of a_j equals $\frac{\hbar K_1}{m}$ and a ‘zero’ indicates that $a_j = \frac{\hbar K_0}{m}$. Therefore 0, 1, 1 implies that $a_1 = \frac{\hbar K_0}{m}$, and $a_2 = a_3 = \frac{\hbar K_1}{m}$, for that scheme. The fluctuating amplitudes in the plots are due to the interference patterns formed by the two waves traveling at two different group velocities. When the waves no longer overlap, such as at $t = 0.2$, the fluctuations are absent (except for any interaction between the slower wave and the absorbing boundary condition).

For the double Gaussian calculations, the range of x over which the reflection ratio, r , was calculated was $[-90..10]$, with the boundaries placed at $x = -90$ and $x = 10$. This placement was necessary to prevent any possible multiple reflections produced by the faster moving distribution from affecting the slower distribution. Also, the two respective reflection waves may be distinguished. The values of the reflection ratio as a function of time is given in Figure 10. Also, for comparison, the values of the reflection ratio at $n = 8400$ ($t = 0.84$) is given in Table 1. At $t = 0.84$, both the initial Gaussian distribution components have passed through the $x = 10$ boundary and only the reflected components are present in the interior domain, and have not yet reached the other boundary. Obviously, when the a_i ’s are tuned to both the initial group velocities, $\hbar K_0/m$ and $\hbar K_1/m$, rather than to just one of these values, the amount of reflection generated by the absorbing boundary conditions drops by up to two orders of magnitude, with the least amount of reflection being produced by scheme 4 in Table 1.

We know from the distribution in momentum space that the initial Gaussians

FIG. 9. Reflection Ratio as a Function of ζ for $K_0 = 15.0$ at $t = 0.3$

No.	Scheme	a_1	a_2	a_3	a_4	time	r
1	Exact implicit	— — —	— — —	— — —	— — —	0.84	5.111×10^{-6}
2	$p = 3$ implicit	$\frac{\hbar K_0}{m}$	$\frac{\hbar K_0}{m}$	$\frac{\hbar K_0}{m}$	— — —	0.84	4.661×10^{-2}
3	$p = 3$ implicit	$\frac{\hbar K_0}{m}$	$\frac{\hbar K_0}{m}$	$\frac{\hbar K_1}{m}$	— — —	0.84	7.364×10^{-4}
4	$p = 3$ implicit	$\frac{\hbar K_0}{m}$	$\frac{\hbar K_1}{m}$	$\frac{\hbar K_1}{m}$	— — —	0.84	1.368×10^{-4}
5	$p = 3$ implicit	$\frac{\hbar K_1}{m}$	$\frac{\hbar K_1}{m}$	$\frac{\hbar K_1}{m}$	— — —	0.84	4.696×10^{-2}
6	$p = 4$ implicit	$\frac{\hbar K_0}{m}$	$\frac{\hbar K_0}{m}$	$\frac{\hbar K_0}{m}$	$\frac{\hbar K_0}{m}$	0.84	2.191×10^{-2}
7	$p = 4$ implicit	$\frac{\hbar K_0}{m}$	$\frac{\hbar K_0}{m}$	$\frac{\hbar K_0}{m}$	$\frac{\hbar K_1}{m}$	0.84	3.295×10^{-3}
8	$p = 4$ implicit	$\frac{\hbar K_0}{m}$	$\frac{\hbar K_0}{m}$	$\frac{\hbar K_1}{m}$	$\frac{\hbar K_1}{m}$	0.84	1.270×10^{-3}
9	$p = 4$ implicit	$\frac{\hbar K_0}{m}$	$\frac{\hbar K_1}{m}$	$\frac{\hbar K_1}{m}$	$\frac{\hbar K_1}{m}$	0.84	8.468×10^{-4}
10	$p = 4$ implicit	$\frac{\hbar K_1}{m}$	$\frac{\hbar K_1}{m}$	$\frac{\hbar K_1}{m}$	$\frac{\hbar K_1}{m}$	0.84	2.394×10^{-2}

TABLE 2

Comparison of Reflection Ratios vs. Different Schemes for Double Gaussian Distribution.

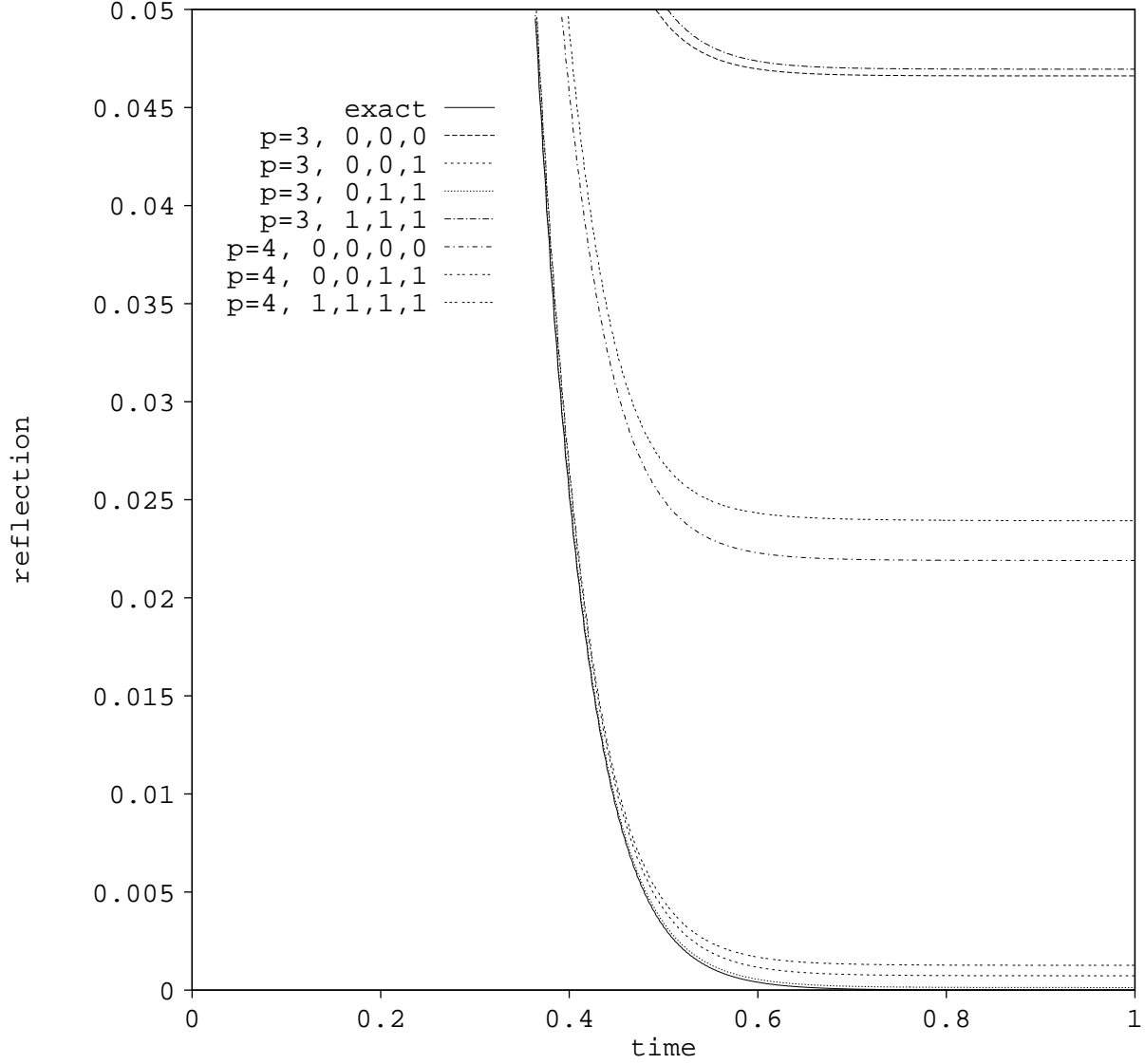


FIG. 10. Reflection Ratio as a Function of Time for Double Gaussian with $K_0 = 25.0$ and $K_1 = 5.0$.

have a distribution in momentum space peaked about $\hbar K_0$ and about $\hbar K_1$. Therefore, for optimal absorbing boundary conditions, the a_j 's that we use should also be distributed around the $\hbar K_0/m$, as well as about $\hbar K_1/m$, to absorb the components that are distributed about $\hbar K_0/m$. So, if we use the same double Gaussian distribution calculation as before but vary the group velocities of the absorbing boundary

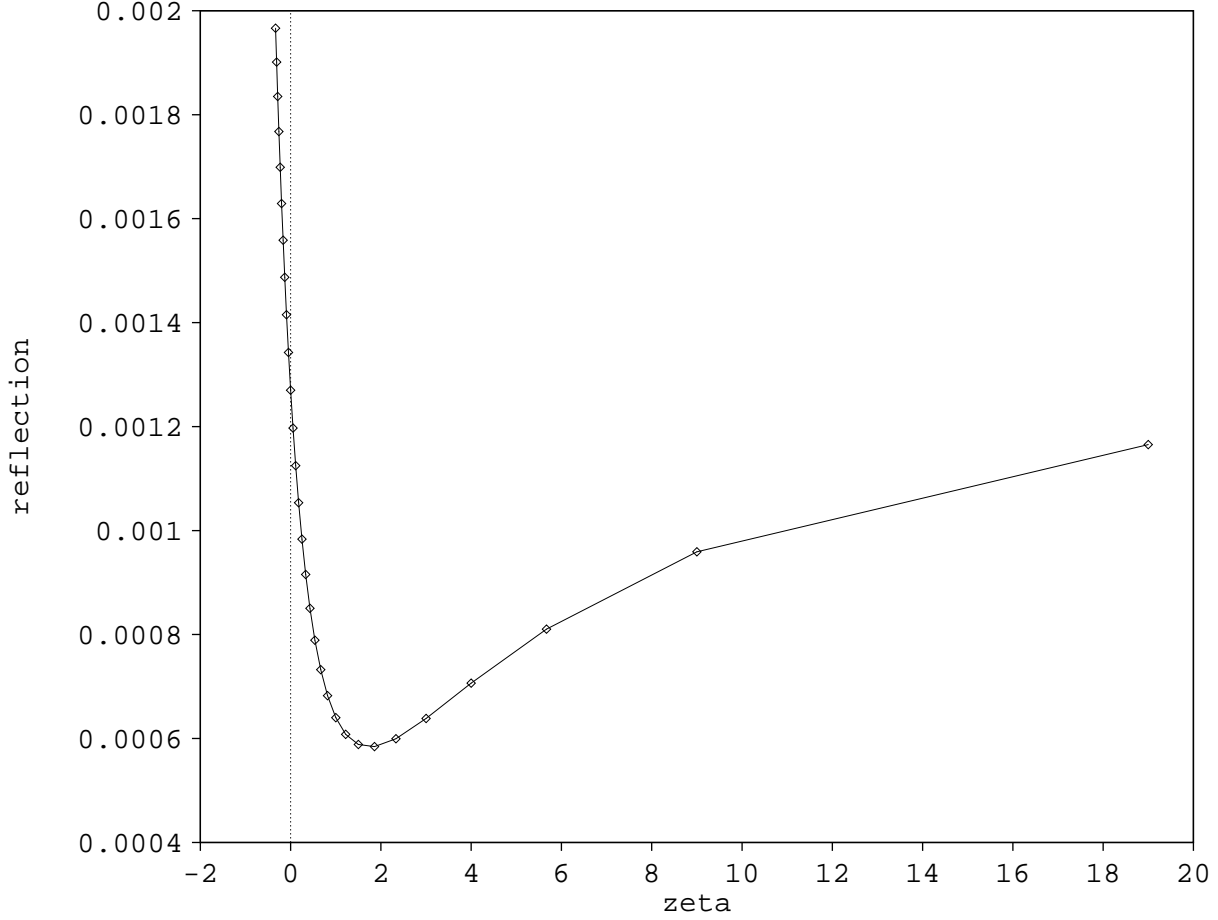


FIG. 11. *Reflection Ratio as a Function of ζ at $n = 8400$ ($t = 0.84$) for Double Gaussian Distribution with $p = 4$ absorbing boundary condition.*

condition for $p = 4$ as follows:

$$(68) \quad a_1 = \frac{\hbar K_0}{m}; \quad a_2 = (1 + \zeta) \frac{\hbar K_0}{m}; \quad a_3 = \frac{\hbar K_1}{m}; \quad a_4 = (1 + \zeta) \frac{\hbar K_1}{m},$$

where ζ is the variation of group velocity, then we obtain the results in Figure 11. We again can see that when a_2 and a_4 are increased, the reflection properties of the $p = 4$ absorbing boundary condition was improved to a peak absorption near $\zeta = 1.8$. Hence, the more spread out the interpolation points of the dispersion relation, the better the performance of the absorbing boundary condition for this initial double Gaussian distribution.

4.3.4. Pseudo-Delta Function Distribution. We would like to also consider the effect of narrowing the spatial spread of the initial Gaussian distribution, and thus having a wider distribution of momentum in momentum space [8]. In particular,

we would like to consider the effect of this modification on the relative reflective properties of the $p = 3$ and $p = 4$ absorbing boundary conditions. Ideally, we would like to consider an initial distribution in the form of a delta function. The definition of a delta function, $\delta(x - x_0)$, is that it have the value 1 at a point x_0 , and be zero everywhere else. As an approximation to a delta function we will use a pseudo-delta function in the form of a Gaussian distribution (65) with $L = 10$, $\sigma_0 = L/100$, and $\xi = 3L/4$. Note that this distribution is one-tenth as wide as the previous Gaussian distributions. As the σ_0 approaches zero, the form of a delta function is recovered. Again, $\delta = 0.0001$ and $\epsilon = L/512$, as before.

We performed calculations i) with no absorbing boundary condition present (i.e., the ideal boundary condition), ii) with a $p = 3$ absorbing boundary condition with $a_i = \hbar K_0/m$, and iii) with a $p = 4$ absorbing boundary condition with $a_i = \hbar K_0/m$. At $t = 1$ ($n = 10000$), these simulations have r values of 2.5959×10^{-2} , 3.1246×10^{-2} , and 2.866×10^{-2} , respectively. Therefore, with the narrower initial spread but wider distribution in momentum space, the $p = 4$ absorbing boundary condition is more effective.

If we use the same pseudo-delta function distribution calculation but vary the group velocities of the absorbing boundary condition for $p = 4$ as follows: $a_1 = a_2 = a_3 = a_4 = (1 + \zeta) \frac{\hbar K_0}{m}$, where ζ is the variation of group velocity, then we obtain the results in Figure 12. The properties displaced in this Figure are different than that for the Gaussian with wider initial spread, σ_0 . Since the Gaussian spreads so quickly as a function of time when evolved by the Schrödinger equation, it turns out that decreased values of a_i lead to a minimized reflection ratio, whereas for distribution with wider initial distributions, the larger values of a_i were more effective.

5. Discussion. For the three types of initial distribution simulations, we find that the higher the order of the absorbing boundary condition, the better the reflection ratio properties (ignoring the essentially equivalent behaviour of the $p = 3$ and $p = 4$ absorbing boundary conditions for a moment). The Dirichlet boundary condition on the other hand produced total reflection of the incident wave. This was not surprising, since the $\Psi = 0$ would have appeared to the wave as a wall of infinite potential value which was impossible to overcome, and thus the wave was completely reflected.

For the single Gaussian distribution, with the momentum being strongly peaked around a single K_0 value, the effectiveness of the $p = 3$ and $p = 4$ absorbing boundary conditions were roughly equivalent. The fact that the $p = 4$ absorbing boundary condition was not more effective for strongly peaked momentum distributions than the $p = 3$ absorbing boundary condition was contrary to our expectations from the reflection ratio value as predicted by Equation (34).

The greater accuracy for the $p = 3$ absorbing boundary condition can be understood in the following sense. In general, the accuracy of an absorbing boundary condition depends on how accurately the interpolation of the dispersion relation models the exact dispersion relation. Hence, for distributions with wide distributions in momentum space, such as for the pseudo-delta function, the $p = 4$ absorbing boundary condition is more effective. And similarly, when there are two or more distinct peaks in the momentum distribution. But when there is only a small distribution in momentum space around the single interpolation point in the dispersion relation, there are other factors that are important. First, of all, the accuracy of the absorbing boundary condition is limited by the consistency error associated with the discretization of the differential operators. Since this error is roughly equivalent for the $p = 3$ and $p = 4$ absorbing boundary conditions, there must also be another factor. This factor stems

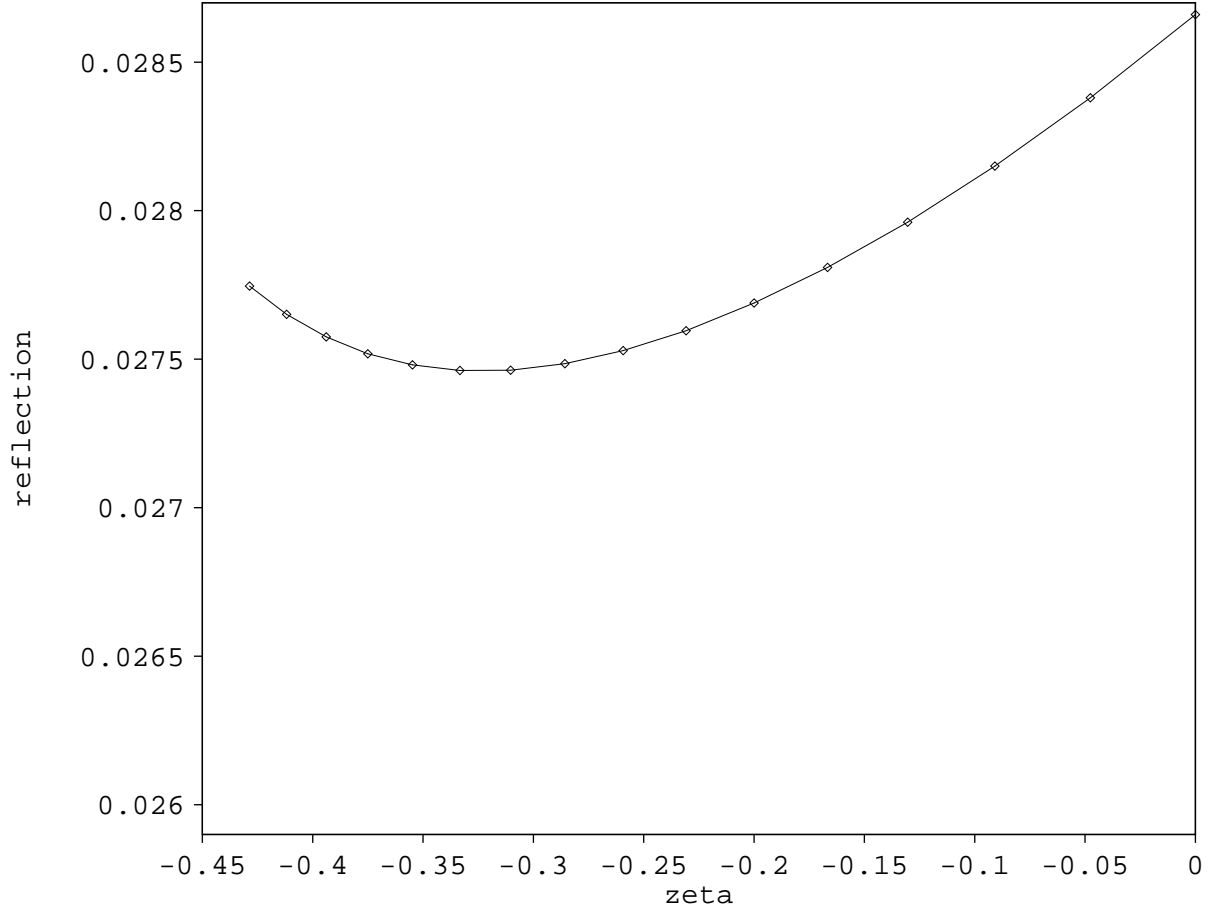


FIG. 12. Reflection Ratio as a Function of ζ at $n = 8400$ ($t = 0.84$) for pseudo-delta function with a $p = 4$ absorbing boundary condition.

from the fact that the absorbing boundary condition admits a generalized eigenvalue with zero group velocity on the boundary, as shown in the previous Chapter. We conjecture that with the higher order absorbing boundary condition may cause this generalized eigenvalue to admit more instability, hence causing the $p = 4$ absorbing boundary condition to be less effective. A similar effect was observed by Higdon for his general absorbing boundary condition for the wave equation, where he states that “the generalized eigenvalue can cause mild instabilities consisting of waves radiating spontaneously into the interior of the boundary” [14]. This behaviour does not seem to effect the overall stability properties of the $p = 4$ absorbing boundary condition. Therefore, for waves which have small momentum spreads about a peak momentum value, the $p = 3$ absorbing boundary condition might be expected to be more effective, whereas for waves with large momentum spreads, the $p = 4$ absorbing boundary condition might be expected to be more effective and the mild instability caused by the generalized eigenvalue is less prevalent. Of course, varying the adjustable parameters

usually improves the behaviour of either.

All the absorbing boundary conditions were more effective at lower values of K_0 (for the range of K_0 presented here), as can be seen from Table 1, which was contrary to the results presented in Kuska's paper [27], whose minimum reflection value appears for $K_0 \approx 15$. Of course, as the values K_0 tend to zero, the dispersion relation has a steeper gradient, and thus the approximations for a fixed order become less accurate. Accordingly, the behaviour of the absorbing boundary conditions will become poorer.

Kuska's results for identical calculations are different than those presented in this paper due to the nature of the cut-off criterion that Kuska used to compare various values of K_0 , where the simulations were terminated when the relation [27] $(\sum_{j=0}^J x |\Psi_j^n|^2) / (\sum_{j=0}^J |\Psi_j^0|^2) < \hat{\epsilon}$ is satisfied. Kuska does not discuss how the value $\hat{\epsilon}$ is determined. Regardless, this cut-off criterion will be insensitive to peculiarities in the behaviour of different waves and it does not account for multiple reflections off different boundaries, whereas as our plateau comparison method does. This is particularly a problem for lower energy waves in a small domain as the reflected wave will be impinging on the opposite boundary before the incident wave has passed completely through the first boundary. Further, due to the nature of Kuska's cut-off criterion, the values of r which Kuska presents are orders of magnitude higher than those presented here, for equivalent schemes (for example, the lowest value for a reflection ratio which Kuska presents is 1.0×10^{-3}). This is due to the choice of a relatively large value of $\hat{\epsilon}$ to accommodate a large range of energies.

Figure 9 shows that the $p = 3$ absorbing boundary condition was more effective for different ranges in momentum space than the $p = 4$ absorbing boundary condition. The $p = 4$ absorbing boundary condition was more effective with larger group velocity values for the parameters of the absorbing boundary condition. These results are related to the forms of the interpolation forms for the absorbing boundary conditions relative to the exact dispersion relation and the evolving group velocity characteristics of the Gaussian distributions.

For the pseudo-delta function, the Gaussian distribution is more sharply peaked, but in momentum space, the momentum distribution is broader. Therefore, when evolved by the Schrödinger equation, the different momentum components cause the distribution to flatten quickly, since the components will be traveling at different velocities. In this case, the $p = 4$ absorbing boundary condition fared better than the $p = 3$ absorbing boundary condition. Thus it can be concluded that the $p = 4$ absorbing boundary condition was effective in reducing the amplitude of components of a wider range of momentum values about a peak value than the $p = 3$ absorbing boundary condition, as discussed above.

But the real power of the general absorbing boundary condition is expressed when used in conjunction with multiple Gaussian distribution with different momentum peaks. This is a more realistic test, since in a practical application, more than one value of K_0 would be expected to be present. Our results are primarily presented by Figure 10. Here the claim that the $p = 4$ absorbing boundary condition is more effective for a wider distribution of momentum values is further illustrated, for the simulations using $a_i = a_j, i \neq j$ for the absorbing boundary conditions. This can be understood from the fourth-order interpolation being a better approximation to the dispersion relation over a wider range of momentum around $\hbar K_0$ in the dispersion relation. Also, when the flexibility of the absorbing boundary conditions is exploited such as the interpolations points are tuned to the two distinct peaks of momentum, $\hbar K_0$ and $\hbar K_1$, the amount of reflection produced by the absorbing boundary conditions is

considerably reduced. Whereas the minimum reflection that an absorbing boundary condition based on Kuska's homogeneous absorbing boundary condition (19) could produce is 4.66×10^{-2} , when the parameters for the $p = 3$ absorbing boundary condition are tuned to both peaks, the reflection ratio falls to 1.37×10^{-4} , a reduction of over two orders of magnitudes. Interestingly, when tuned to the momentum peaks, the $p = 3$ absorbing boundary condition again proved more effective than the $p = 4$ absorbing boundary condition (again probably due to the mild instability associated with the generalized eigenvalue), although the latter allows for one more adjustable parameter which could be useful for even more general incident waves.

To summarize, the absorbing boundary conditions are effective choices for boundary conditions where the boundary must not interfere with the interior solution, unlike the standard Dirichlet boundary condition. The general absorbing boundary condition developed in this thesis is flexible enough to be adapted for a wide range of incident waves, either with multiple group velocities and/or with wide distributions in momentum space, while producing a minimal amount of reflection.

REFERENCES

- [1] A. Bayliss and E. Turkel, *Radiation boundary conditions for wave-like equations*, Comm. Pure Appl. Math **33** (1980), 707–725.
- [2] Jan Broeze and Edwin F.G. Van Daalen, *Radiation boundary conditions for the two dimensional wave equation from a variational principle*, Mathematics of Computation **58** (1992), no. 197, 73–82.
- [3] R.W. Clayton and B. Engquist, *Absorbing boundary conditions for wave equation migration*, Geophysics **45** (1980), 895–904.
- [4] Dale R. Durran, Ming-Jen Yang, Donald N. Slinn, and Randy G. Brown, *Toward more accurate wave-permeable boundary conditions*, Monthly Weather Review **121** (1993), 604–620.
- [5] Bjorn Engquist and Andrew Majda, *Absorbing boundary conditions for the numerical simulation of waves*, Mathematics of Computation **31** (1977), no. 139, 629–651.
- [6] ———, Comm. Pure Appl. Math. **32** (1979), 313.
- [7] Ian Galbraith, Yin Sing Ching, and Eitan Abraham, *Two-dimensional time dependent quantum-mechanical scattering event*, American Journal of Physics **52** (1984), no. 1, 60–68.
- [8] Abraham Goldberg, Harry M. Schey, and Judah L. Schwartz, *Computer-generated motion pictures of one-dimensional quantum-mechanical transmission and reflection phenomena*, American Journal of Physics **35** (1967), no. 3, 177–186.
- [9] B. Gustafsson, H.-O. Kreiss, and A. Sundström, Math. Comput. **26** (1972), 649.
- [10] G. Ronald Hadley, *Transparent boundary condition for beam propagation*, Optics Letters **16** (1991), no. 9, 624–626.
- [11] ———, *Transparent boundary condition for the beam propagation method*, IEEE Journal of Quantum Electronics **28** (1992), no. 1, 363–370.
- [12] Charles A. Hall and Thomas A. Porsching, *Numerical analysis of partial differential equations*, Prentice Hall, 1990.
- [13] Mark Hedley and M.K. Yau, *Radiation boundary conditions in numerical modeling*, Monthly Weather Review **116** (1988), 1721–1736.
- [14] Robert L. Higdon, *Absorbing boundary conditions for difference approximations to the multi-dimensional wave equation*, Mathematics of Computation **47** (1986), no. 176, 437–459.
- [15] ———, *Initial-boundary value problems for linear hyperbolic systems*, SIAM Review **28** (1986), no. 2, 177–217.
- [16] ———, *Numerical absorbing boundary conditions for the wave equation*, Mathematics of Computation **49** (1987), no. 179, 65–90.
- [17] ———, *Radiation boundary conditions for elastic wave propagation*, SIAM Journal of Numerical Analysis **27** (1990), no. 4, 831–870.
- [18] ———, *Absorbing boundary conditions for elastic waves*, Geophysics **56** (1991), no. 2, 231.
- [19] ———, *Absorbing boundary conditions for acoustic and elastic waves in stratified media*, Journal of computational physics **101** (1992), no. 2, 386.
- [20] ———, *Radiation boundary conditions for dispersive waves*, SIAM Journal of Numerical Analysis **31** (1994), no. 1, 64.

- [21] M. Israeli and S.A. Orszag, *Approximation of radiation boundary conditions*, Journal of Computational Physics **41** (1981), 115–135.
- [22] Hong Jiang and Yau Shu Wong, *Absorbing boundary conditions for second-order hyperbolic equations*, Journal of Computational Physics **88** (1990), no. 1, 205–231.
- [23] J.B. Keller and D. Givoli, *Exact non-reflecting boundary conditions*, Journal of Computational Physics **82** (1989), 172–192.
- [24] R.G. Keys, *Absorbing boundary conditions for acoustic media*, Geophysics **50** (1985), no. 6, 892–902.
- [25] R. Kosloff and D. Kosloff, *Absorbing boundaries for wave propagation problems*, Journal of Computational Physics **63** (1986), 363–376.
- [26] H.-O. Kreiss, *Initial boundary value problems for hyperbolic systems*, Comm. Pure Appl. Math. **23** (1970), 277–298.
- [27] J.-P. Kusk, *Absorbing boundary conditions for the Schrödinger equation on finite intervals*, Physical Review B **46** (1992), no. 8, 5000–5003.
- [28] Wilbert Lick, Kirk Ziegler, and James Lick, *Interior and boundary difference equations for hyperbolic difference equations*, Numerical Methods for Partial Differential Equations **2** (1986), 157–172.
- [29] ———, *Open boundary conditions for hyperbolic equations*, Numerical Methods for Partial Differential Equations **3** (1987), 101–115.
- [30] E.L. Lindman, *‘free-space’ boundary conditions for the time-dependent wave equation*, Journal of Computational Physics **18** (1975), 66–78.
- [31] Kenneth K. Mei and Jiayuan Fang, *Superabsorption - a method to improve absorbing boundary conditions*, IEEE Transactions on Antennas and Propagation **40** (1992), no. 9, 1001–1010.
- [32] M.J. Miller and A.J. Thorpe, *Radiation conditions for the lateral boundaries of limited-area numerical models*, Quarterly Journal of the Royal Meteorological Society **107** (1981), 615–628.
- [33] Daniel Neuhasuer and Michael Baer, *The time-dependent schrödinger equation: Application of absorbing boundary conditions*, Journal of Chemical Physics **90** (1989), no. 8, 4351–4355.
- [34] I. Orlanski, *A simple boundary condition for unbounded hyperbolic flows*, Journal of Computational Physics **21** (1976), 251–269.
- [35] R.A. Pearson, *Consistent boundary conditions for numerical models of systems that admit dispersive waves*, J. Atmos. Sci. **31** (1974), 1481–1489.
- [36] W.H. Raymond and H.L. Kuo, *A radiation boundary condition for multi-dimensional flows*, Quarterly Journal of the Royal Meteorological Society **110** (1984), 535–551.
- [37] R.A. Renaut, *Absorbing boundary conditions, difference operators, and stability*, Journal of Computational Physics **102** (1992), 236–251.
- [38] R. Sakamoto, *Hyperbolic boundary value problems*, Cambridge University Press, New York, 1982.
- [39] Tsugumichi Shibata, *Absorbing boundary conditions for the finite-difference time-domain calculation of the one-dimensional Schrödinger equation*, Physical Review B **43** (1991), no. 8, 6760–6763.
- [40] A. Sommerfeld, *Partial differential equations in physics*, Academic Press, 1949.
- [41] Lloyd N. Trefethen, *Group velocity in finite difference schemes*, SIAM Review **24** (1982), no. 2, 113–136.
- [42] ———, *Group velocity interpretation of the stability theory of Gustafsson, Kreiss and Sundström*, Journal of Computational Physics **49** (1983), 199–217.
- [43] Lloyd N. Trefethen and L. Halpern, *Well-posedness of one-way wave equations and absorbing boundary conditions*, Math. Comput. **47** (1986), 421–435.
- [44] Edwin F.G. Van Daalen, Jan Broeze, and Embrecht Van Groesen, *Variational principles and conservation laws in the derivation of radiation boundary conditions for wave equations*, Mathematics of Computation **58** (1992), no. 197, 55–71.